POLITECNICO DI TORINO

Automotive Engineering
Master Degree

Master Degree Thesis

Ultra-lightweight vehicle hydraulic transmission and concept development

Relator

prof. Massimo Rundo

Candidate

Simone Sarpedo

Accademic year 2021-2022

Ringraziamenti:

Voglio ringraziare con queste poche righe le persone che più mi hanno accompagnato durante questi anni.

Anhelina, per il supporto costante e per il tempo dedicato a spronarmi.

Due parole anche alla mia famiglia ed agli amici, per l'aiuto e per la condivisione di questa fatica.

Infine, voglio ringraziare il professor Rundo, per la profonda pazienza mostrata nei miei confronti.

Mi auguro, ora, di poter finalmente intraprendere nuovi interessanti percorsi. Forte delle esperienze fatte.

Alla prossima…

Simone

Abstract

The document reports the steps taken during the study of a hydraulic transmission for bicycles, which came with the proposal to verify feasibility from outside Politecnico of the simulation model made. The aim was to demonstrate that the project could be functional and had the characteristics necessary for use on bicycles.

The structure of the 3D model provided was first studied and the documentation provided led us back to the operating principle that we wanted to pursue. Later, similarities were sought with existing projects for which there are studies performed, to better understand the possible criticalities.

The analysis started from the original system and extrapolated the key features to ensure operation. It was concluded that the system did not have the characteristics necessary for operation; therefore, the systems were dimensioned to ensure the operation, as far as possible without altering the original idea.

Finally, alternatives have been developed and varied to the project to demonstrate the possibility of realization even with different operating principles, but equally effective. By adding the possibility to add additional features and functionalities if it is considered necessary for the purpose of completeness of the final product.

Index

List of Figures

1. Development proposal Introduction

The aim of this study is to document the steps that have taken during the development of the project proposal, the latter, presented to the DENERG Energy Department by a body outside the university. The proposal required the feasibility study of a hydraulic transmission applied to ultralight vehicles, specifically: bicycles.

The peculiarity of this proposal is the adoption of a rotating masses system mounted on the wheel hub that, subject to the centrifugal force given by the wheel rotation speed, can adjust the displacement of the pump or hydraulic motor, obtaining the variation of the transmission ratio.

The project, already in the patent application phase, presented a three-dimensional digital model with all the dimensioned components, in figure 1 you can view the exploded system. A complete feasibility study could be carried out using the data provided. It used spreadsheets to simulate the forces and displacements of the kinematic control system, while the Amesim program was used to simulate the fluid dynamics of the transmission.

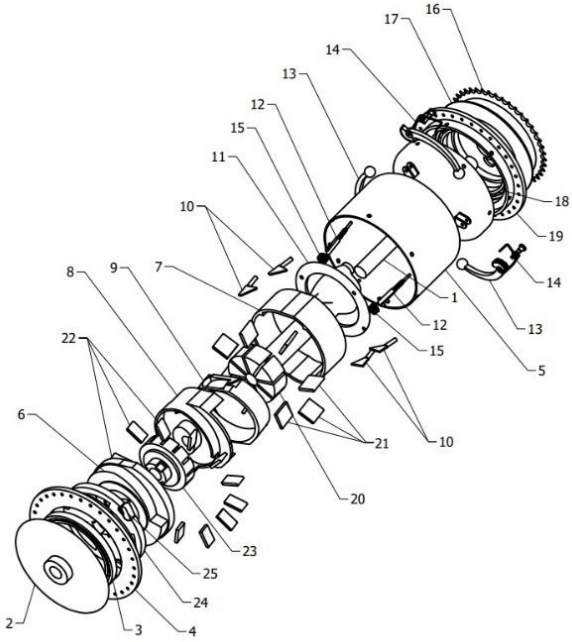

Figure 1: Explosion of wheel hub from patent description

The first steps will be made in the study of the state of the art of similar solutions adopted over time, even on vehicles and applications different from the final goal, to better understand the solutions and get the best possible product. Subsequently, a descriptive model of the development proposal will be transposed on the different systems, in order to be able to directly simulate the behaviour at the different operating conditions, these last ones will be developed in order to obtain as much information as possible.

To simplify the analysis, it was decided to divide the system into two macro-assemblies: the first concerning the regulation system, including all those parts suitable for the movement of the stator of the hydraulic machine; while the second, including the hydraulic machines of the system. Schematizing in figure 2 the circuit that was presented to the department.

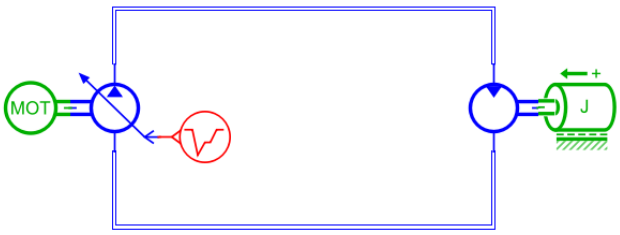

Figure 2: Hydraulic transmission scheme

The basic principle of operation uses a simplified closed-circuit hydraulic transmission, therefore, consisting of a hydraulic pump and motor connected directly to each other. From the documents and description provided by the source: there was the intent to vary the displacement of the pump, or you provide the alternative to vary the displacement of the hydraulic motor, to vary the ratio of total transmission. The actuation is, instead, automatic and in function of the speed of rotation, taking advantage of the centrifugal acceleration of rotating masses. Structured like that it would allow to accommodate the entire block in the wheel hub, making it in fact an accessory easily installed to any bicycle with the simple replacement of the rear wheel. In figure 3 you can see the wheel hub with the holes in the wheel spokes housing and the crown to receive the motion of the pedaling through chain; you can also see part of the system with rotating masses.

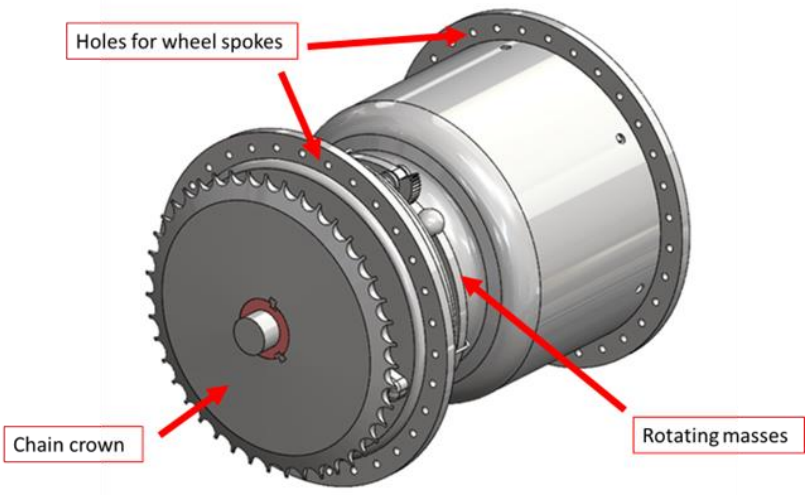

Figure 3: Wheel hub

The proposal lacks data demonstrating its functionality, but it does allow for some reflection on the application of hydraulic principles to ultralight vehicles.

The realization of a hydraulic transmission includes a pump and a motor connected by two lines: high and low pressure. Assuming to maintain a single direction of rotation, when the load reverses the direction there is the inversion of the pressure on the two branches, passing from the flow power from motor to load, to have the load that provides the power and generates the flow towards the primary motor; in figure 4 the variation of the pressure on the hydraulic lines is shown at the change of direction of the power flow. By nature of the vehicle must never present the condition of reversal of motion; therefore, it will not be taken into account as a case of operation, but the type of transmission would make it theoretically possible.

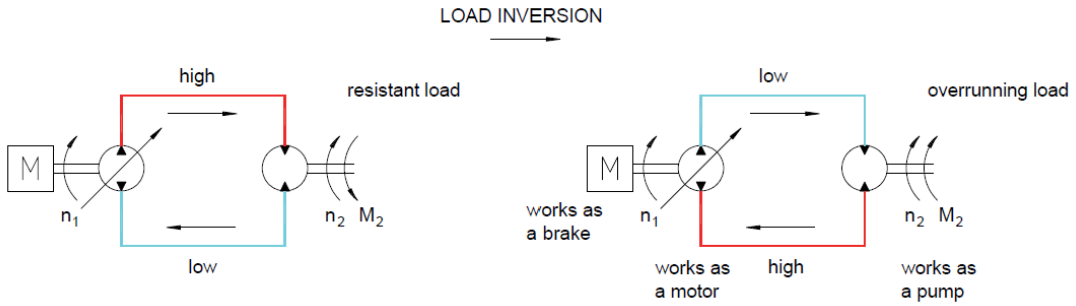

Figure 4: Power direction change and its effect on lines pressure

The aim of the project is to create a machine that can improve comfort at varying speeds without the direct intervention of the cyclist. Thus, creating an automatic transmission with continuous transmission.

Looking at the three-dimensional model provided, it was noted that the motor has an unusual stator profile, shown in figure 5 below; without the possibility of creating an accurate simulation model, it was therefore decided to adopt standard solutions to simulate easily the system reducing the study variables. From an initial estimate, was led to think that the transmission of drive power occurs using high pressures and low flow rates, consequence of the adoption of hydraulic machines with reduced volumes and subject to the rotation regime of a wheel without intermediate transmission ratios. In addition, the control mechanism, implemented by centrifugal acceleration, brings with it peculiar geometries and a long chain of actuation components, which will need to be verified to ensure proper regulation.

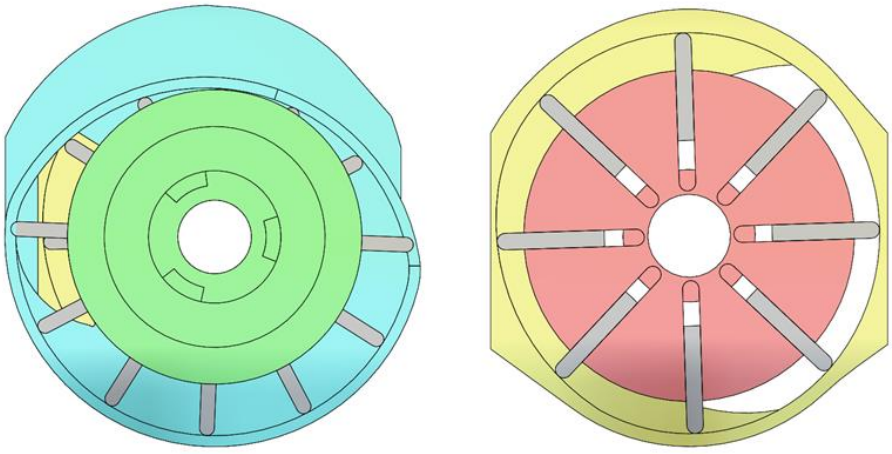

Figure 5: Hydraulic motor on left, Pump on right at zero displacement

2. State of art

The idea of getting an alternative transmission to the chain for a bicycle was studied for some time now. Specifically, there are countless patent proposals focused on the hydraulic transmission; some equipped, simply, by a pump to the pedals and by a hydraulic motor to the wheel, as proposed by the figure 6 deriving from an old American patent, others instead focused on the realization of a continuous transmission.

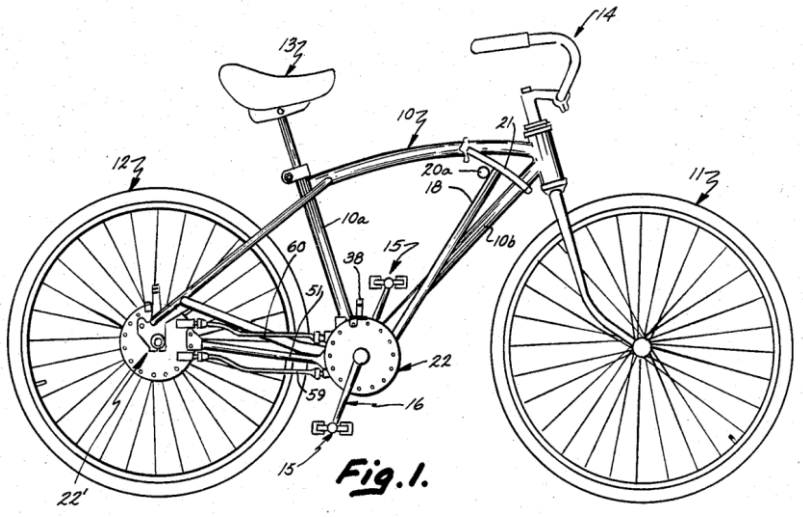

Figure 6: Hydraulic transmission of patent US4546990 of 1985

As the main case study of ideas regarding hydraulic drive bicycles was chosen a modern model designed by students, who called the prototype made "PurdueTracer", which is named from the name of the university where it was developed. The objective was the realization of an energetically efficient human-powered hydraulic bicycle, whose main characteristic is the adoption of an electro-actuated open circuit for regulation, partly different from the project proposal, but equally relevant. The interesting aspect of this project remains the choice of hydraulic lines depending on the operating condition of the system. For example, the presence of a hydraulic motor dedicated to the transmission of driving power during pedaling, which has a different circuit during the energy release phase, for example, after a regenerative phase in braking.

The scheme of figure 7 has been extracted from the official documentation of the presentation of the project, which illustrates the principles of operation: the pump "P" on the left is connected via a gear transmission to the pedals of the cyclist, which puts pressure on the system and starts the motor "M"; to increase the flow rate was added an auxiliary pump "HP", on the right of the diagram, the synergy of the two pumps and with the opening of the valve "V2" At the top you have the intention to charge the accumulator in case of need; Finally the pump "RP" is able to slow down the vehicle during braking starting the phase called regeneration, "RP" is also this time connected with a gear transmission and connected to the wheel by means of a clutch, which is necessary to disengage the pump outside the regeneration phases.

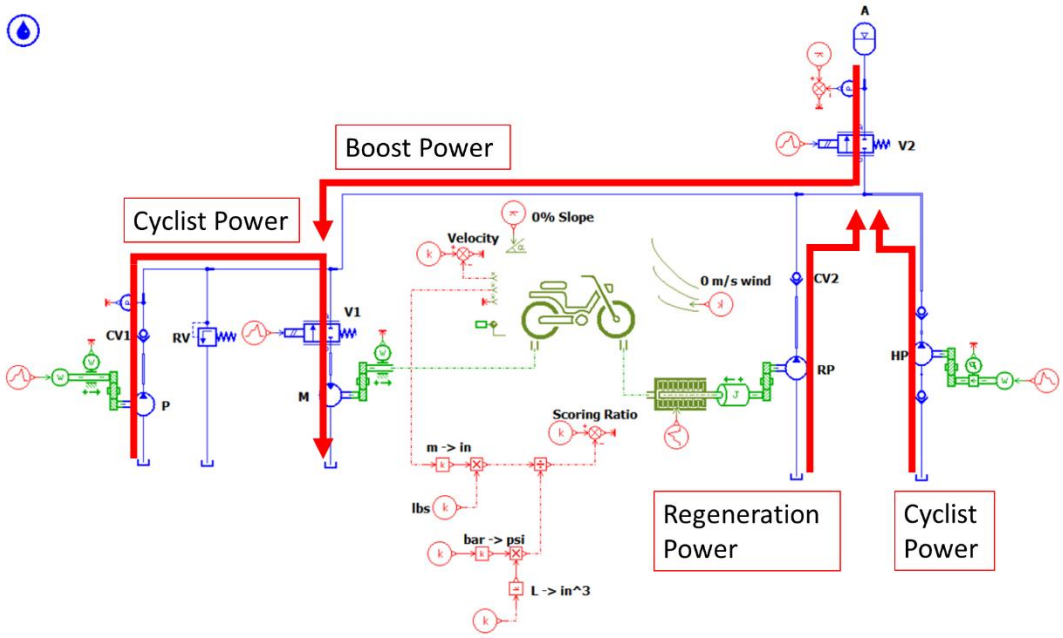

Figure 7: PurdueTracer Scheme and Power flow

The second proposal which is in mention is another bicycle with hydraulic transmission called "OYO chainfree bike" in development by B.C. Bike. The proposal combines the concept of assisted pedaling to a hydraulic transmission, thus taking advantage of the versatility of a hydraulic circuit to mechanically decouple the electric motor and wheel. The system has a pump and a motor on a closed circuit with electric servo assistance, ensuring a variable continuous transmission quite similar to the project here on study, in picture 8 it shows the arrangement. The hydraulic machines used belong to the category of volumetric machines with fixed displacement with radial pistons, capable of generating high pressures even at low speeds.

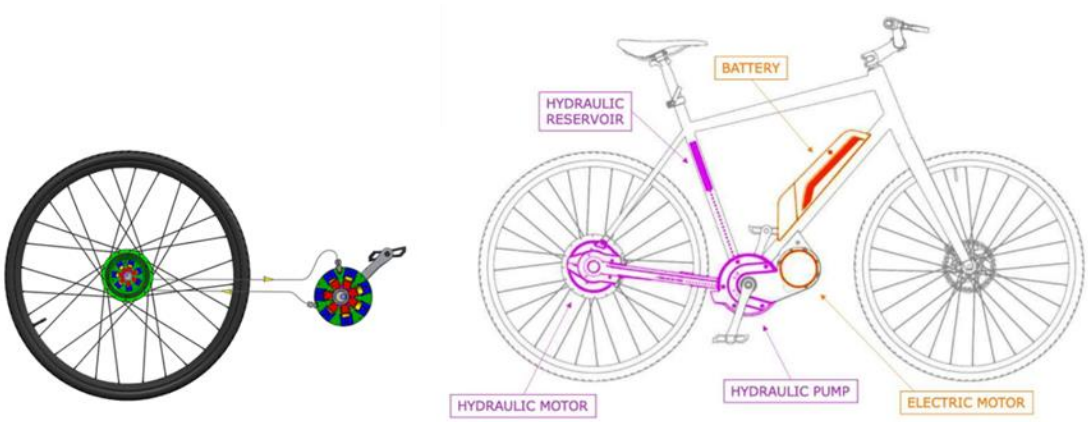

Figure 8: OYO chainfree bike

The proposal submitted for study is in the middle between the two solutions presented. It incorporates the closed circuit of the OYO bike, but with the implementation of simpler hydraulic machines, valves for directing the fluid and an accumulator.

3. Development

Now that there is a general view of the project and an understanding of similar applications, there is the intention to proceed with the verification study of the product submitted. Analysing separately the two macrosystems already seen: the regulation mechanism with centrifugal actuation and the hydraulic transmission.

3.1 Mechanism with Centrifugal movement actuation

The regulation subsystem is entirely developed by focusing the principle of centrifugal force applied to a complex mechanism, composed of levers and kinematic systems geometrically constrained by adjustment calibration which is to be obtained.

3.1.1 Geometric evaluation

The complete kinematic chain comprises many components that would transform the centrifugal force into a translation perpendicular to the rotation. This arises from the need to have a pump stator movement or motor stator to get the displacement change. This solution is one of the many possible alternatives, we proceed in this way with the aim of studying the entire system under study, which is shown in all its components in image 9.

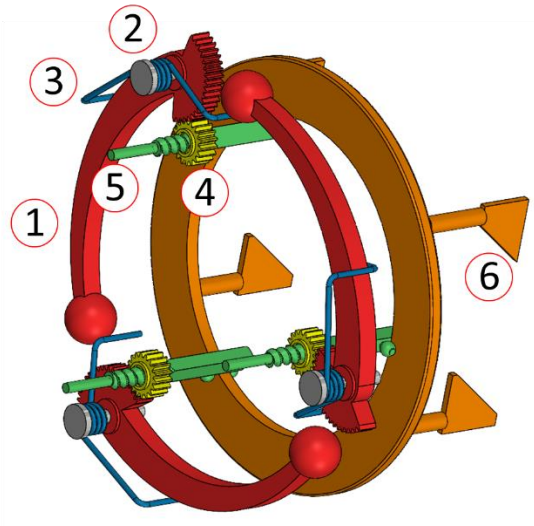

Figure 9: All components of centrifugal control system

The trigger for the movement of the entire mechanism originates from the concentrated masses located at the end of the external levers (1), which are hinged to the wheel hub by means of a pin (2), shown in section in image 10. Then, at the same speed of rotation, you will get more

torque to the hinge as the masses or arm increase. In addition, the need to open the levers depending on the available space and the necessary displacement to be evaluated.

The adoption of this principle should ensure a precise lever position in relation to a specific vehicle speed. Next, it should be noted that the position of the lever is given by the balance of forces between the torque resulting from the centrifugal force and the torque given by the angular spring, mounted on the hinge (3). At reduced speeds, the spring will ensure the return of the lever in the collected position with a force dependent by the preload condition.

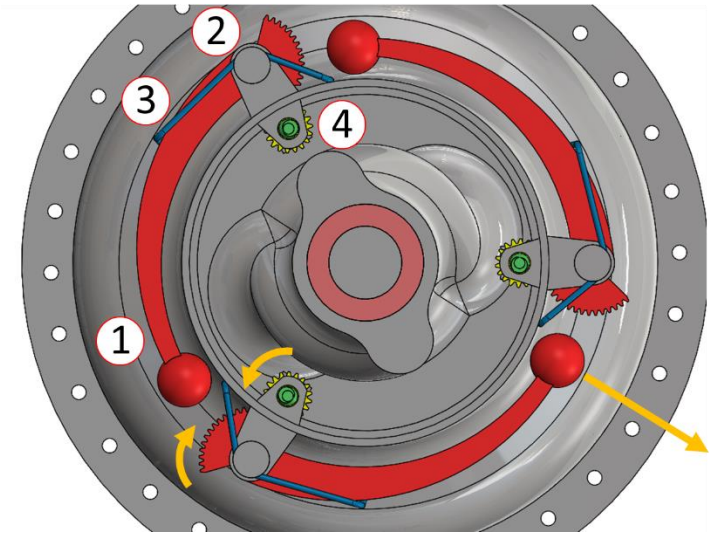

Figure 10: Wheel hub rotation axis section

Following the kinematic chain there is now a pair of gears with a reduction factor of less than one, necessary to increase the rotation angle of the driven wheel (4). This last one is axially constrained as shown in figure 11, having the only degree of freedom of rotation, which will allow the axial translation of the thrust rod (5) with the help of a non-standard threaded profile, maximizing thrust in the presence of a limited angle of rotation. Finally, with the adoption of opposing inclined planes (6) the position of the stator (7) of the pump varies, in the image 12.

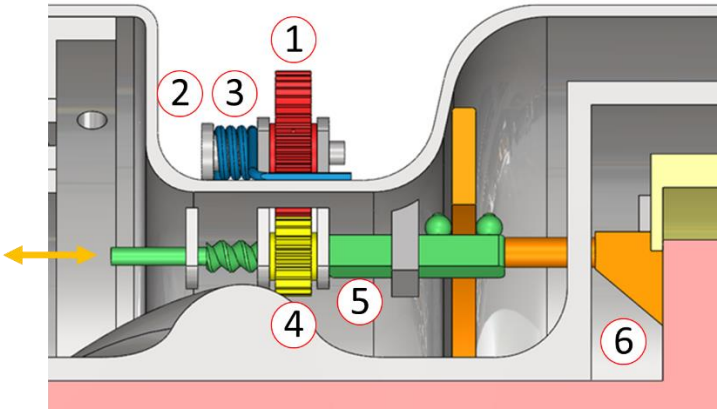

Figure 11: Wheel hub along rotation axis section

Among the other components there is a "disc", which has the purpose of interfacing the levers through the thrust rods and the inclined planes of displacement adjustment; in a real application

it would have the objective of synchronizing and redistributing the forces between the internal components of the system, coordinating the thrust forces and ensuring the degree of freedom of rotation of the hub with respect to the pump stator, necessary to decouple the stator reaction forces. During the calculations will be considered simply as a friction and therefore an inefficiency.

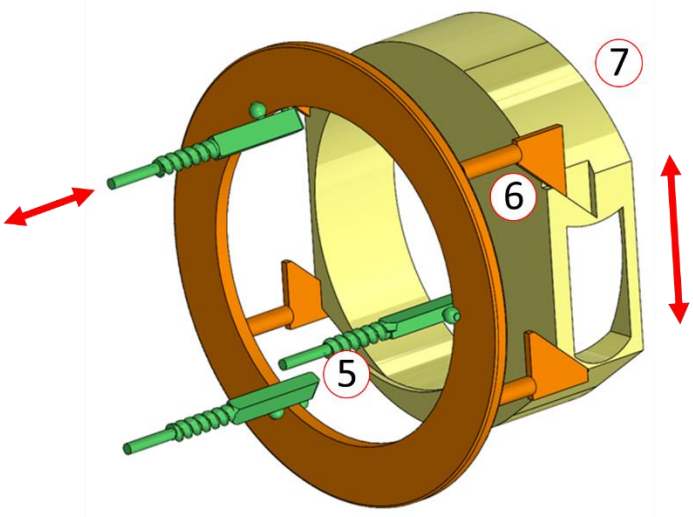

Figure 12: Stator pump interface

We want to immediately implement a variation to the project, replacing the pump with a moving stator with a rotating stator pump. The choice is given by a necessary simplification and reduction of the number of components. This will vary the stator translation interface, which will no longer have opposing inclined planes, but there will be only one inclined plane which interposed between wheel hub and stator will rotate the stator around its hinge and then varying its displacement. The advantages are to be sought: in a greater stability of the stator, which will be less subject to displacement and therefore to oscillations of the displacement; in the forces of implementation, which are concentrated in a single inclined plane; in the least number of components, leading to a lower malfunction coefficient, in addition to having less surface friction and therefore inefficiencies. Picture 13 shows the difference between a moving stator pump, such as the one in the three-dimensional model, and a hinged stator pump at point O.

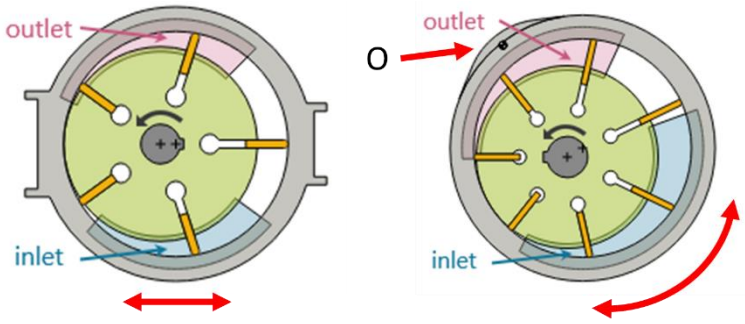

Figure 13: Translating vs Rotating Pump stator configuration

3.1.2 Actuation forces calculation

The actuation chain was verified in two spreadsheets. One for the calculation of the forces acting on the lever and one for the analysis of the forces and displacements, necessary for the verification of feasibility.

Taking as reference a hydraulic transmission with only the variable displacement vane pump, the minimum force for the displacement of the stator was calculated. The actuation force has the same direction but opposite to the spring elastic force which allows the stator to return to the resting condition. Also the result of the internal pressures to the chambers of the pump generates a result shown in image 14, which has the direction that oscillates in the time in function of the rotor rotation and therefore of the chambers in pressure; chambers, passing from the suction zone to the compression and discharge zone, changes the pressure sign overcoming the axis of application of external forces. Imagining that the rotor rotates counter clockwise, the positive pressure will be in the upper area of the axis mentioned, in conjunction with the pump discharge. In addition, it is specified that the resultant pressure oscillation has discontinuities, generated by the connection of the pressurized chambers with the flow, as well as the connection of a chamber to the suction.

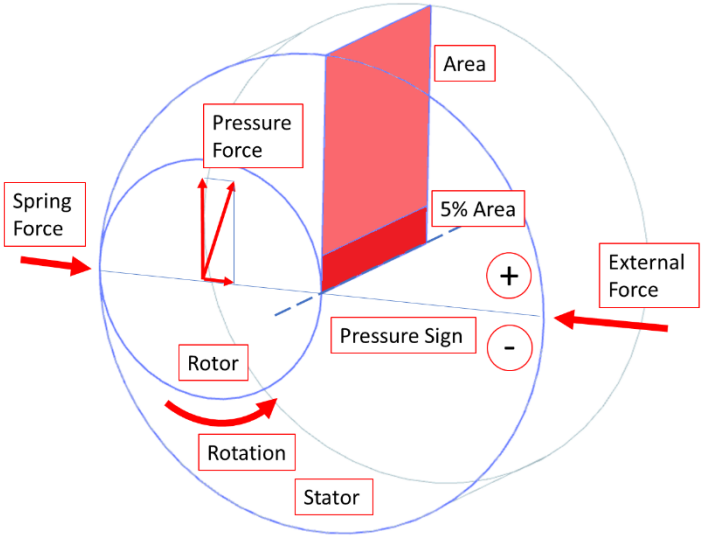

Figure 14: Empiric calculation representation

Thus, it is necessary to minimize the effect of the generated counter-adjustment of the internal forces of pressure. Knowing the principle of operation of the pump has calculated, empirically, the needed force F_{dist}, which will be large enough to not allow the counter spontaneous adjustment during the rotation of the rotor.

Equation 1:

$$F_{dist}\ [N] = p_m * H * R_{stat} * 0{,}05$$

Where: p_m is the average pressure in chambers, H is the width of the chamber and R_{stat} the internal stator radius.

The formula number 1 calculates the force as the product of 5% of the application area for the mean positive pressure in the pump chambers.

Since the studies of hydraulic transmission and control system have been carried out in parallel, here it is possible to show an extraction of data that will be commented on later in the section 3.2.2 dedicated to transmission:

p_m	12	bar
H	25	mm
$R_{stat} = D_{stat}/2$	70	mm

Table 1 - Brief pump geometry description

From calculation of equation 1: $F_{dist} = 105\ [N]$

To carry out the feasibility test is needed to obtain F_{dist} in the made spreadsheets and the formulas generated are in function of components geometry inside the kinematics. By entering and checking iteratively with the torque data generated by the opening of the levers with rotating masses, results were obtained that allowed to calculate the force of thrust greater than F_{dist}. Small geometric corrections were made to the original model in order to obtain results with a greater margin.

The last iteration was carried out is shown, which led to a solution with a thrust force on the stator greater than F_{dist}.

Has been estimated the force F_{dist} into the maximum opening condition of counter-weight lever, where the angle $\vartheta_{max} = 130\ [°]$, the total mass $m = 0{,}1\ [kg]$ and the lever length $R = 0{,}15\ [m]$, the mass generates a force of $F_{max,130}$ = 12 [N], which is multiplied to the arm projection "b" on perpendicular plane of r', generates 0,63 [Nm] into hinge O'. Entities shown into picture 15. Is also calculated corresponded speed of the force v = 24 [km/h], calculated with the rotation speed ratio between masses on lever and wheel hub equal to one.

Equation 2:

$$F_{max,130} = m * r' * \omega^2 = m * r' * \left(\frac{v}{3{,}6} * \frac{2}{D_{wheel}}\right)^2$$

Where: D_{wheel} is the diameter expressed in meters of a 29" wheel, a standard size for bicycles.

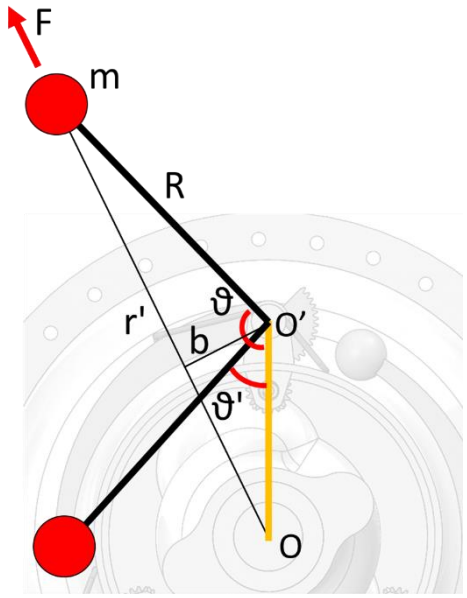

Figure 15: Maximum lever aperture

Subsequently, the gears couple allows to increase the angle of rotation to the disadvantage of the torque that becomes of $T_{max,\ out}$ = 0,221 [Nm]; the thread hole in pinion gear converts the rotation into translation, which generates a thrust of F_n = 277 [N]; finally obtaining a push on the stator, through the inclined plane, of about F_{act} = 160 [N]. In addition, the influence of friction has been estimated, overall quantified with a factor equivalent to η_{tot} = 0,85 [-], thus reducing the thrust to $F_{act,\ net}$ = 135 [N]. Sufficient force as estimated above.

New weight	m	0,1	kg
Centripet force @130°	F_{max}	12	N
Arm	R	0,15	m
Centripet arm @130°	r'	0,35	-
Max Torque at gear	$T_{max,\ in}$	0,630	Nm
Reduction ration gear	i	0,35	-
Max torque at pinion	$T_{max,\ out}$	0,221	Nm
Radius pinion thread	r_{th}	3,25	mm
Force pinon tangential	F_{th}	67,8	N
Thread Pitch	p_{th}	5	mm
Angle	α_{th}	13,76	°
Slope	α_{th}	0,97	%
Force Normal	F_n	277,1	N
Angle of stator actuator	α_{st}	60	°
Force tangential of stator	F_{act}	160,0	N
Spur gear eff	η_{gear}	0,98	-
Thread eff	η_{th}	0,90	-
Sliding Surfaces	η_a	0,98	-
Sloped plane	η_s	0,98	-
Overall eff	η_{tot}	0,85	
Resultant force on stator	$F_{act,\ net}$	135,5	N

Table 2: Full results

Equation 3:

$$T_{max,in} = F_{max} * R * r'$$

Equation 4:

$$T_{max,out} = T_{max,in} * i$$

Equation 5:

$$F_{th} = \frac{T_{max,out}}{r_{th}} * 10^3$$

Equation 6:

$$\alpha_{th} = \tan^{-1}\left(\frac{P_{th}}{r_{th} * 2 * \pi}\right) * \left(\frac{180}{\pi}\right)$$

Equation 7:

$$F_n = F_{th} * \cot\left(\alpha_{th} * \frac{\pi}{180}\right)$$

Equation 8:

$$F_{act} = F_n * \cot\left(\alpha_{st} * \frac{\pi}{180}\right)$$

Equation 9:

$$F_{act,net} = F_{act} * \eta_{tot} = F_{act} * \eta_{gear} * \eta_{th} * \eta_a * \eta_s$$

Moreover, it is necessary to obtain a sufficient stator displacement to allow the displacement change. The objective is Δx_{stator} = 6 [mm], achieved thanks to geometrical corrections: considering an overall opening of the lever of $\Delta\vartheta$ = 85°, gear ratio of i = 0,35 [-], thrust rod thread pitch of p_{th} = 5 [mm] and an inclined plane of α_{st} = 60° is obtained the translation of $\Delta x'_{stator}$ = 5,84 [mm]. Considered sufficient because the objective is to be considered as a guideline and not as a minimum necessary threshold.

Overall moving angle Gear	$\Delta\vartheta$	85	°
Reduction ration gear	i	0,35	-
Overall moving angle Pinion	β	243	°
Radius pinion thread	r_{th}	3,25	mm
Thread Pitch	p_{th}	5	mm
Angle	α_{th}	13,76	°
Rod movement	Δx_{rod}	3,37	mm
Angle of stator actuator	α_{st}	60	°
Stator movement	$\Delta x'_{stator}$	5,84	mm
Goal	Δx_{stator}	6	mm

Table 3: Calculated traslation

Note that in tables the values highlighted in yellow are the results of the calculations, in white the values entered.

Equation 10:

$$\Delta\vartheta = \vartheta_{max} - \vartheta'$$

Equation 11:

$$\beta = \frac{\Delta\vartheta}{i}$$

Equation 12:

$$\Delta x_{rod} = P_{th} * \frac{\beta}{360}$$

Equation 13:

$$\Delta x'_{stator} = \Delta x_{rod} * \tan\left(\alpha_{st} * \frac{\pi}{180}\right)$$

With the original geometrical values the forces were sufficient, but at the same time the displacements were less than 2 [mm] and therefore largely insufficient for the purpose. As shown in table 4 below.

Overall moving angle Gear	85	°
Reduction ration gear	0,35	-
Overall moving angle Pinion	243	°
Radius pinion thread	3,25	mm
Thread Pitch	2,5	mm
Angle	6,98	°
Rod movement	1,69	mm
Angle of stator actuator	45	°
Stator movement	1,69	mm
Goal	6	mm

Table 4: Calculated translation with original geometry

3.1.3 Regulation

The previous calculation allowed to find the necessary torque, so that the translation of the stator is sufficiently wide and with a sufficient high force to counteract the resulting pressures. Now we want to verify that the total of weights and levers is able to generate the principle of adjustment. Which puts in relation the speed of rotation with the desired displacement; schematizing the assembly you can get the result in the following figure 16.

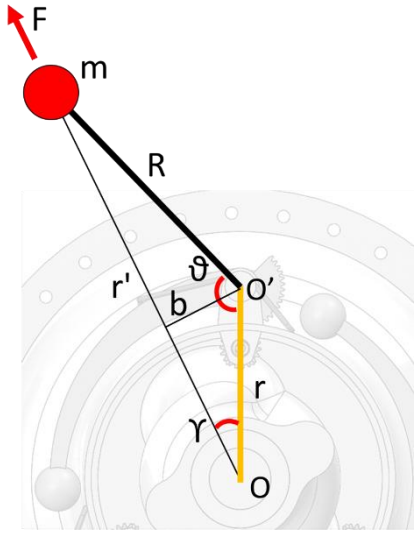

Figure 16: Lever Angles

There are three main actors: the hub, which remains stationary with respect to the reference system in O; the lever, hinged in O'; the concentrated mass, mounted at the end of the lever. The centrifugal force is applied to the mass and passed through the centre O.

The centrifugal force has a quadratic trend as a function of the speed of rotation, which multiplied to the arm generates a "driving" torque T_m. Considering the total masses applied on a single lever, obtaining an equivalent system.

Equation 14:

$$T_m = m * \omega^2 * r' * b$$

Where: m is the total mass, ω is the wheel hub rotating speed, r' is the rotating radius of the mass, b is the force application arm, O is the centre of the wheel hub, O' is the hinge of the mass lever and R is the length of the mass lever. In the picture 16 "r" represents the distance between the centre of rotation O and the hinge O' on which the lever is mounted.

In addition, was sought a geometric combination that would make the centrifugal force adjustable, as much as possible, with the spring's linear elastic force. Dictated by the need to obtain the position of the lever linearly proportional to the displacement change. Through an iterative process has been reached a deviation from the linearity of 10% maximum.

R	150	mm
r	90	mm
m	0,1	kg
D_{wheel}	725	mm
i_m	7	-

Table 5: Geometric lever and wheel data

Where: i_m is the gear ratio between the wheel and the hydraulic motor.

The spring preload has been set considering that the lever can remain in the fully retracted position up to a speed of 8 [km/h], while at lower speeds there is no need to change the transmission ratio. The choice allows you to better distribute the adjustment range over a narrower speed range, potentially more accurately. In addition, the presence of a preload makes the lever system less sensitive to external shocks and vibration provided by the vehicle in motion.

Preload	2,49	Nm
Spring rate	0,35	Nm/°

Table 6: Spring characteristics

The opening angle of the lever is between θ_{in} = 90° and θ_{fin} = 140° in function of the longitudinal vehicle speed, compared to the previous calculation of opening angle $\Delta\vartheta$ has been further reduced, because forces were higher than the previous calculation condition and for the necessity to regulate the lever opening with the radial spring, the reduction of the lever opening favours the coupling between spring and lever from the torque point of view. In addition, we consider a bicycle with 29-inch wheels and the adoption of a speed multiplier (i_m interposed between motor and wheel, to increase the centrifugal force.

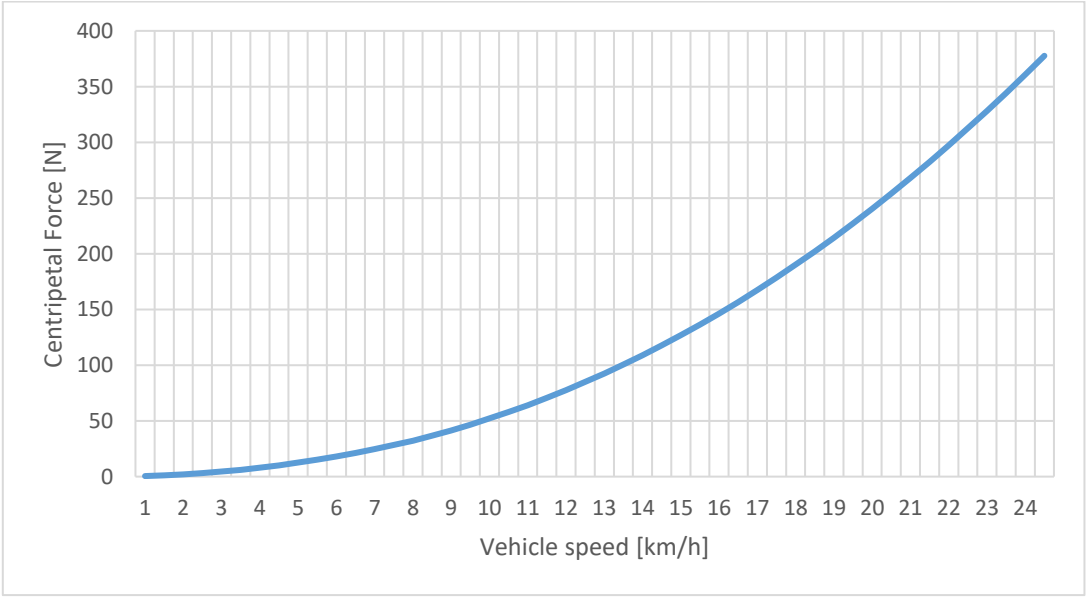

Figure 17: Quadratic behaviour of centrifugal force

Another phenomenon that occurs is the variation of the projection of the arm with which the torque generated by the centrifugal force is calculated. The opening of the lever as a function of speed is measured with the angle Theta around the hinge in O'; higher the speed, means greater angle Theta, but at the same time the gamma angle will decrease, gamma is proportional to the projection of the lever b.

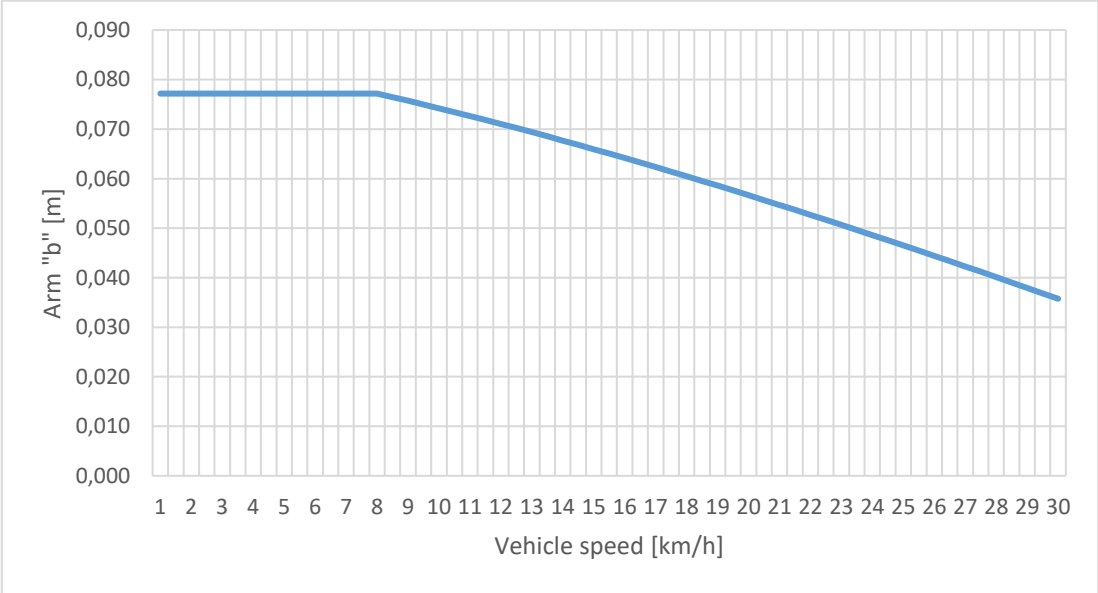

Figure 18: Arm "b" dimension behaviour in function of vehicle speed

Equation 15:

$$\omega_{hub}[RPM] = \frac{v * 60 * i_m}{3{,}6 * D_{wheel} * \pi}$$

Equation 16:

$$r' = \sqrt{\left(R^2 + r^2 - 2 * R * r * \cos\left(\vartheta \frac{\pi}{180}\right)\right)}$$

Equation 17:

$$\gamma = \sin^{-1}\left(\frac{R}{r'} * \sin\left(\vartheta * \frac{\pi}{60}\right)\right) * \frac{180}{\pi}$$

Equation 18:

$$b = r * \sin\left(\gamma * \frac{\pi}{180}\right)$$

Equation 19:

$$F_{cent.} = m * \left(\omega_{hub} * \frac{2\pi}{60}\right)^2 * r'$$

Equation 20:

$$T_{cent.} = F_{cent.} * b$$

Equation 21:

$$T_{preload} = T_{cent} \text{ @ } 8\ [Km/h]$$

Equation 22:

$$K_{spring} = \frac{T_{cent} \text{ @ } 30\ [Km/h] - T_{cent} \text{ @ } 8\ [Km/h]}{\vartheta_{max} - \vartheta_{min}}$$

Equation 23:

$$T_{spring} = T_{preload} + \left(K_{spring} * (\vartheta - \vartheta_{min})\right)$$

Where: ω_{hub} is the rotating speed of the wheel hub on which are mounted the lever masses, $F_{cent.}$ is the applied force on equivalent mass, $T_{cent.}$is the lever torque with equivalent mass on hinge, $T_{preload}$ is the spring preload, K_{spring} is the spring elastic constant, T_{spring} is the torque generated by the spring.

The result obtained is visible in figure 19, which shows that it is possible to have a sufficiently precise adjustment for angles between 90° and 120°; corresponding to vehicle speeds up to 20 [km/h]. Beyond which there are deviations from the linearity more relevant, but still acceptable.

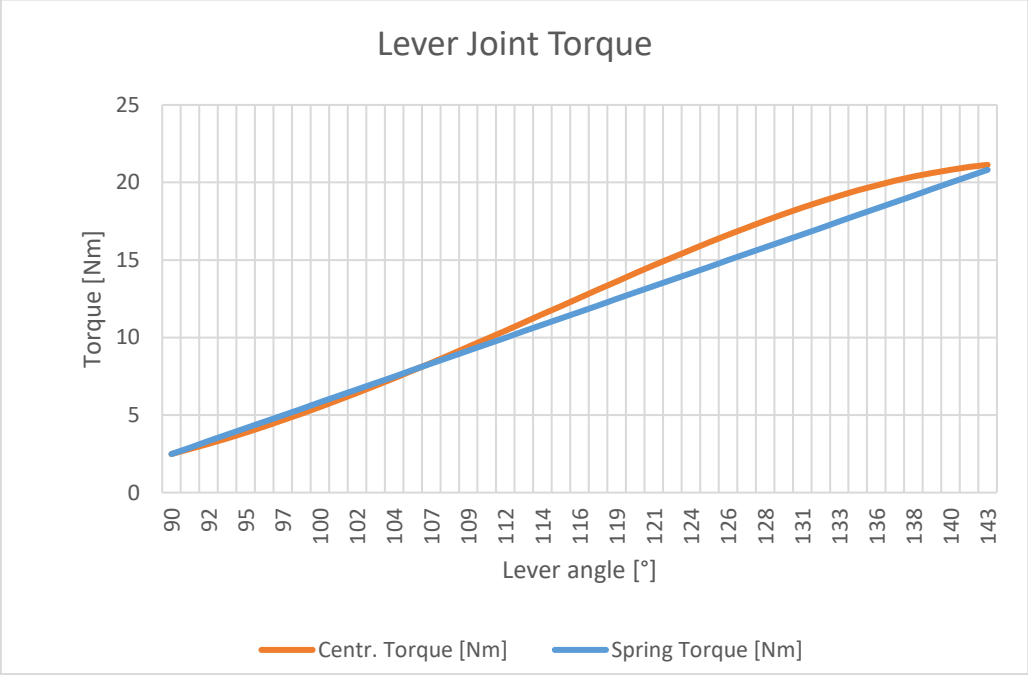

Figure 19: Centrifugal and spring Torque

To conclude the impact on the variation of the lever system, it was decided to verify again how much the error influenced the calculation of the angle Theta, calculated from the amount of torque necessary to the balance:

Equation 24:

$$T_{Useful} = T_{Centr.} - T_{Spring} - (K_{Spring} * \Delta\vartheta)$$

Where: T_{Useful} is the useful torque generated, $T_{Centr.}$ Is the centrifugal torque given by the rotating mass, T_{Spring} is the spring preload, K_{Spring} is the elastic spring constant, $\Delta\vartheta$ is the difference between the initial angle (in this case 90°) and the given angle for the specific speed.

The result was again divided by the spring's elastic constant to find the error of the angle difference that would affect that specific travel speed:

Equation 25:

$$\Delta\vartheta_{error} = \frac{T_{Useful}}{K_{Spring}}$$

Finally, the percentage of error in the calculation was calculated as:

Equation 26:

$$\Delta\vartheta_{error}\,[\%] = \frac{\Delta\vartheta_{error}}{\Delta\vartheta}$$

The value of theta along the entire range of compatible speeds with the vehicle operation varies from a minimum of -1% to a maximum of +4%. To obtain a more accurate result is necessary to reinserting the correct values of Theta instead of the theoretical values of Theta and performing one or more iterations. By the nature of the study, it was decided not to continue further and to focus on the next point of development.

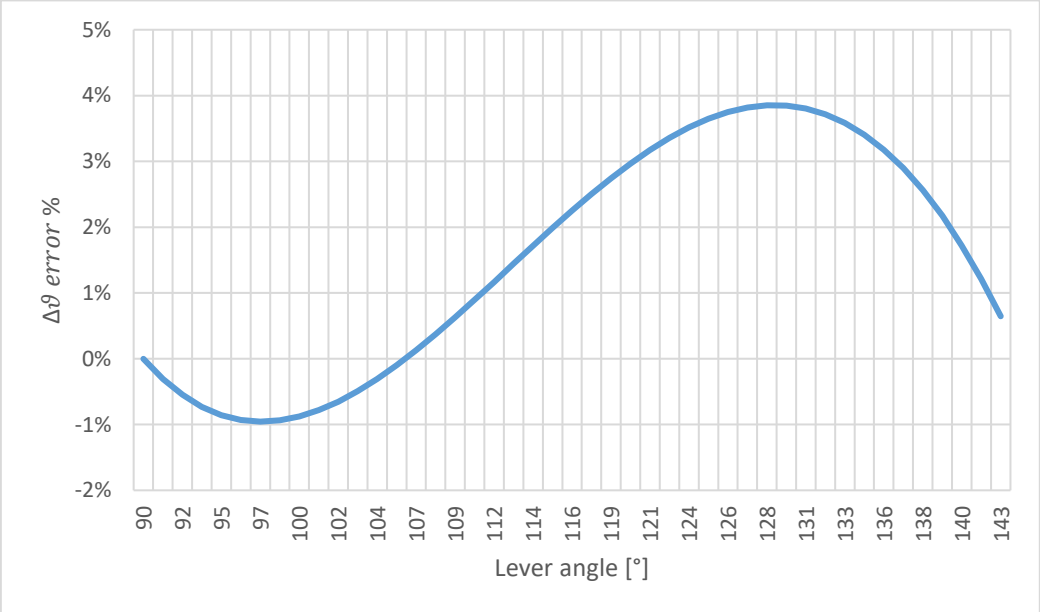

Figure 20: Error angle calculation

3.1.4 Considerations

From an initial analysis it can be said that the idea is conceptually simple, reliable and effective, but they reserve doubts about the possible reliability on the real counterpart; as vibrations, friction and wear over the time can quickly deteriorate the goodness of the project.

Despite this, the calculations show some scope for improvement and optimization of geometries, but in view of a use in a real environment has more than one criticality:

- Friction and constant maintenance required on hinges and other contact surfaces
- Weight is potential high
- Moving part are exposed
- Difficulty calibration (but necessary), depending on the habits of the end user (speed and effort for the displacement change)
- Needed of accurate engineering

Assuming use in a controlled environment, the functionality of the mechanism can be confirmed.

Among the advantages surely are found in the materials used, economic and easy to find, as well as easily achievable.

3.2 Bicycle transmission

The hydraulic transmission, generally used on special energy conversion applications, has been chosen for this application thanks to its great versatility; on the other hand, it results in reduced efficiency due to leakage and fluid friction. In order to minimize the negative aspects and maximize the benefits, it was decided to make the simulations progressively more complex and accurate through the simulation software Amesim.

3.2.1 Simplified model for development and critical displacements

The project submitted to the study, presents hydraulic machines with reduced displacements that, actually, at reduced rotational speeds generate minimum flow rates. In order to generate suitable speed for the cyclist for an average use of a bicycle, he must develop a specific flow rate and pressure at hydraulic motor, equivalent to a net transmitted power expressed by the next formula:

Equation 27:

$$P\,[W] = V\left[\frac{m^3}{rev}\right] * n\left[\frac{rev}{s}\right] * p\,[\,Pa\,]$$

Where: P is the generated power, V is the revolution displacement of the hydraulic machine, n is the rotating speed and p is the generated pressure.

Specifically, if the cyclist decides to maintain a specific speed, this means that the system will provide a very specific power. If is now decided to vary the displacement, and therefore the flow, inevitably will also change the pressure on system in order to maintain the same transmitted power. Thus, assuming to transmit 300 [W] with the assumption of machines efficiency equal to one:

Equation 28:

$$p\,[\,Pa\,] = \frac{P[W]}{\left(V\left[\frac{m^3}{rev}\right] * n\left[\frac{rev}{s}\right]\right)} = \frac{300}{\left(\frac{20}{10^6} * 1\right)} = 1'500'000\,[Pa] = 150\,[bar]$$

With a motor displacement of V = 20 $\left[\frac{cc}{rev}\right]$, a gear reduction ratio between motor and wheel $i = 1\,[-]$ and a rotating speed of pedals $n = \ 60\,[rpm] = 1\,[\frac{rev}{s}]$, there will be pressures of $p = \ 150\,[bar]$ into hydraulic circuit.

The pressure found by the previous formula, if applied to the circuit, would lead to an inevitable strengthening of the components of the whole system; with the consequent increase in weight and a lower volumetric efficiency due to internal leakages. With the above consideration it is decided, therefore, to adopt larger displacements, leading to two benefits: first, reduce the pressure to adopt hydraulic machines less resistant and therefore potentially lighter components; consequently, increase the flow rate, keeping the power transmissible by the transmission and improve the volumetric efficiency of the machines. The balance between pressure and flow will be checked during the simulation.

Some consideration about real hydraulic machines are made during the model simulation realisation, such as internal and external drawing, which are immediately included into modelling: internal and external leakages. Which would lead to an inexorable emptying of the circuit. Thus, the first proposed scheme will already be equipped with an auxiliary internal line, which will have the function of collecting the fluid that escapes from the main line through external leakages and restoring the correct amount of fluid in the circuit for proper system operation. Another consideration that are needed to apply already concerns the storage system to ensure the minimum pressure on the low-pressure circuit. Necessary to avoid zero or even negative pressure conditions during the simulation, which in a real application would give rise to cavitation phenomena.

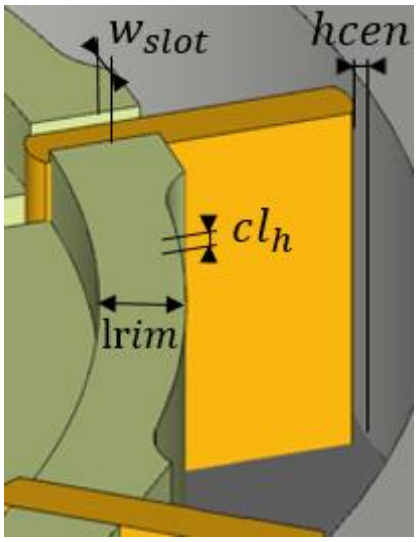

Figure 21: In vane pump, some dimensions which generate leakages

The motor and the pump have internal leakages, which are simulated by estimated volumetric efficiency at the moment. That is a simple performance factor, currently set to 0.8 [-]. While the external leakages are simulated by the orifice "lamorif" in figure 22, with representative values of: height $h = 0{,}01\ [mm]$, width $w = 0{,}5\ [mm]$ and depth $l = 1\ [mm]$; Thus, the leakages, will be collected at low pressure on the internal line and stored with the accumulator; in addition to serving the circuit in case of overpressure or depression. The accumulator is now set to pressure $p = 20\ [bar]$.

Equally important is the choice of fluid to be adopted, set in "elementaryhydraulicrops" in figure 22. A sufficiently viscous fluid was chosen due to the fact that the circuit will have reduced flow rates and rotation speeds, further reducing the phenomenon of leakage. The chosen oil is the ISO VG 68 oil - Mobil DTE 68; while the average operating temperature is set to 60 [C.].

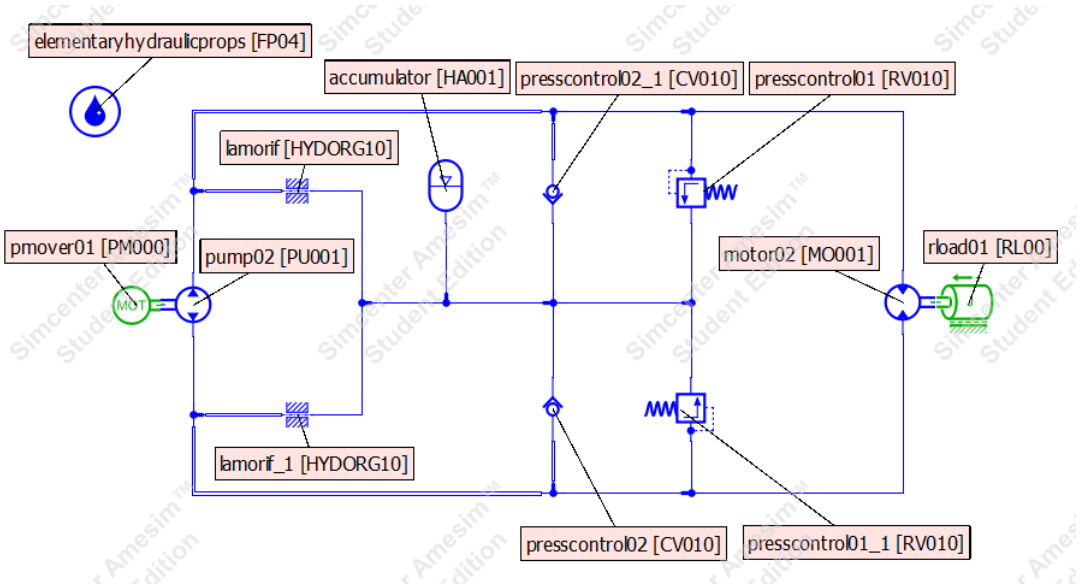

Figure 22: Preliminary hydraulic transmission scheme

In summary, the boundary conditions for the next steps will be:

- Low rotating speed
- At least on machine at variable displacement
- Need of low operating pressures to limit the system weight
- Intention to maintain a traditional cycling feeling

To overcome, at least in part, the first condition, have been adopted gearboxes with high conversion factors, between pedals and pump in a ratio of 1:10, between motor and wheel 7:1. This choice will considerably improve the hydraulic performance without greatly affecting the mechanical performance.

The hydraulic machines choice was based on their simplicity balanced with efficiency. The variable displacement vane pump and a gerotor motor. The pump, due to the need to have a variable displacement machine and to keep the simulation similar to the original idea proposed, has kept the original adoption, a vane configuration. As for the motor led to a different choice, as a gerotor motor turns out to be overall simpler.

It was decided that the adoption of both variable displacement machines was not necessary, as there would be no significant benefits, but also a more complex system. The configuration to primary variable, the case studied, corresponds to the part of diagram "constant torque", while the variable secondary configuration would correspond to the curves "constant power"; of course, if both hydraulic machines were variable displacement, they would have the possibility to work in the areas underlying the curves of the graph in image 23, considering to have a constant pedaling speed and constant delta pressure.

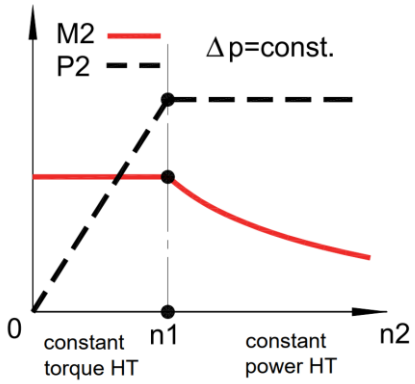

Figure 23: Hydraulic transmission behaviour with pump and motor variable displacement

The configuration with the primary variable only allows to use the transmission at different speeds and consequently at different powers. The second configuration would be useful only in the event that you arrive at maximum power, but there was still the need to get to higher travel speeds; as we will see later this condition will never occur during the normal use of a bicycle.

By testing different motor and pump configurations, a compromise of operation is achieved with the following values: Pump displacement V_p, Motor displacement V_m, Pump reduction ratio i_p and Motor reduction ratio i_m.

V_p	100	cc/rev
V_m	50	cc/rev
i_p	0,1	-
i_m	7	-

Table 7: New pump and motor: displacement and reduction ratio

Where the reduction ratio: $i = \frac{\omega_{in}}{\omega_{out}}$

The advantages of this configuration, as already mentioned, come in the greater balance between pressures and ranges at the same transmitted power. The adoption of speed reducers was necessary to increase the rotational speeds of the hydraulic pump and motor, otherwise too low to ensure proper operation. As proof of the assumptions made in the introduction, where it was anticipated that too small displacements and inadequate rotation speeds lead to having to raise the pressures up to hundreds of bars for the transmission of the motion of a

bicycle. Recalculating the pressure generated with the new parameters gives the maximum pressure of the circuit significantly improved. $p = 15\ [bar]$.

Subsequently, it was decided to refine the simulation related to the accumulation system. The accumulator considered is the "spring" type because it is very simple and varing the accumulated fluid there is a linear variation of the pressure. In addition of needing to ensure the storage of sufficient fluid to the circuit, it has the aims to ensure a minimum pressure on the low line, preventing the phenomenon of cavitation at the pump.

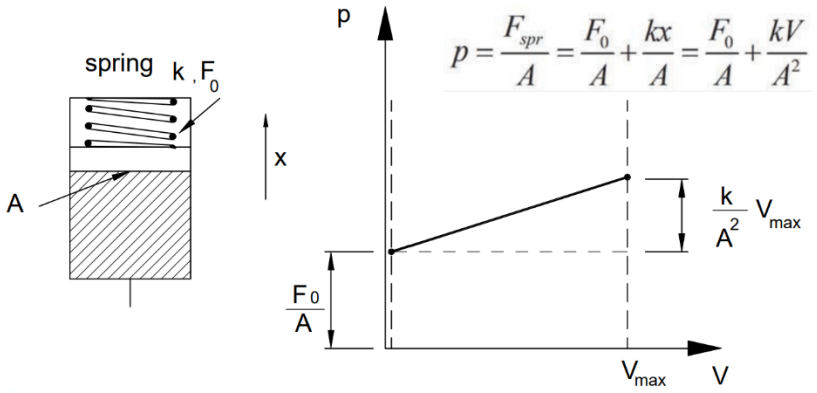

Figure 24: String accumulator behaviour

As is easily to predict: as the diameter increases, the internal pressure will be reduced with the same force applied to the plunger. In addition, the spring has a preload function, which force is multiplied by the surface and define the minimum pressure to implement the plunger P_{min}. Useful in order to identify the empty system condition and to ensure a minimum amount of fluid even at very low pressures. The maximum pressure, instead, is calculated as the surface product of the plunger for the sum of the preload and the force given by the total compression of the spring. This value must never be reached during normal conditions of use, because a lot reached, the accumulator will no longer be able to accommodate other fluid and then will be generated pressure peaks potentially harmful to the system.

Moreover, the volume must be sufficient during all phases of operation, because there will be conditions of greater demand and phases of release or expansion of the fluid.

Diameter	Dacc	100	mm
Stroke	Sacc	20	mm
Spring Preload	-	100	N
Spring ratio	k	700	N/mm
Min Pressure	Pmax	0,13	bar
Max Pressure	Pmin	17,95	bar
Volume	Vacc	157,08	cm^3

Table 8: Spring accumulator geometry

The values in the table were consolidated after having confirmed that there were no negative pressure or saturation conditions of the accumulator, even during simulations of increased stress.

3.2.2 Development of optimized models for pump and hydraulic motor

The basic model is now no longer sufficient to study the behaviour of the machines; therefore, it is necessary to deepen the knowledge of the functioning of the machines. Realization of detailed geometric and efficiency models, with subsequent equivalent transposition on the overall model of the system. In addition, optimized pump and motor profiles similar to real models are adopted; applied to unfavourable and more stressful operating conditions for the system, represented by the development of maximum power and flow in conditions of maximum slope or speed. The collected data will be used to indicate the margins of use of the project and any changes aimed at improvement.

The first machine to change the simulation model is the gerotor hydraulic motor. It has already been mentioned its adoption, but never describing its structure. The gerotor is equipped with two rotating parts: the first is the internal rotor, in the center connected to the drive shaft of the motion equipped with six teeth in the current case; the second is the external rotor, equipped with sectors equal to the number of teeth of the internal rotor plus one, in this case seven, the rotation of the second rotor takes place around a different axis of the rotating shaft, allowing to vary the volume of the spaces between the two rotors depending on the angle of rotation. Both rotors are contained inside the stator, which aims to distribute and collect the fluid through the openings on the sides. To obtain approximately the displacement Vm = 50 [cc/rev] the following values were adopted in Table 9.

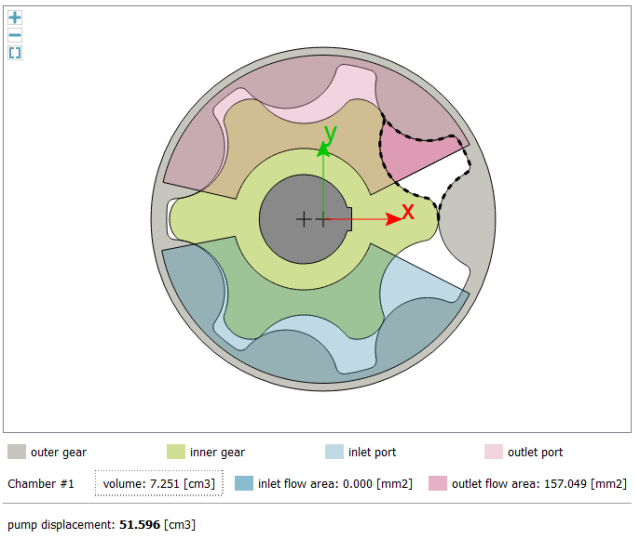

Figure 25: Gerotor profile

Number of teeth on ext. gear (z)	7	-
Trochoid generating radius (K)	41,7	mm
Radius of circular arcs of ext. gear (S)	13	mm
Radius of circle to complete ext. gear (G)	39	mm
Eccentricity (ecc)	4,8	mm
Radius of fillets on ext. gear (rf)	2	mm
Gear thickness (H)	26	mm
Inlet port start angle	191	°
Inlet port final angle	333	°
Outlet port start angle	27	°
Outlet port final angle	167	°

Table 9: Gerotor model parameter

To simulate the leakages and flows, at this point in the study, it is no longer enough to use theoretical parameters, but it is necessary to use specially made models, among these are the modules: "vecvarlamorif" which simulates internal leakages in function of the angle and redistributing the flow in the adjacent chambers through "vecflowredirect", as in figure 26. While, the external flow is not a function of the rotation so flow through "vecvarorif" set at constant value.

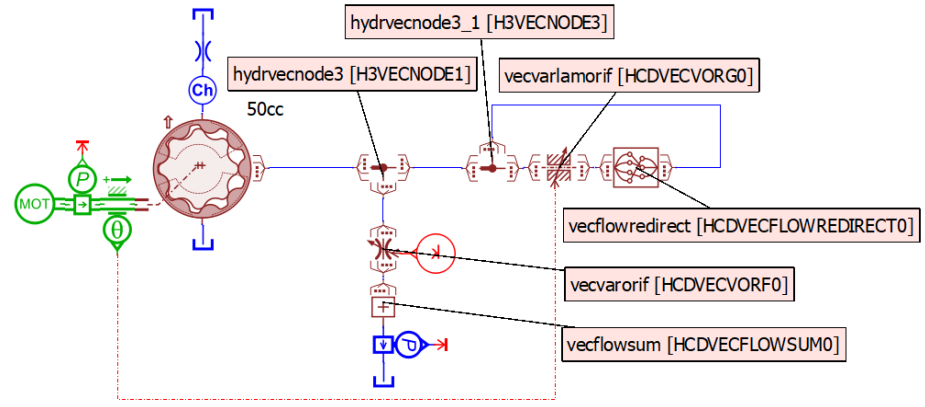

Figure 26: Complex Gerotor lekages model

The module "vecflowredirect" then allows to assign a sector of memory to each value in the vector, which will be reassigned progressively according to the angle of rotation.

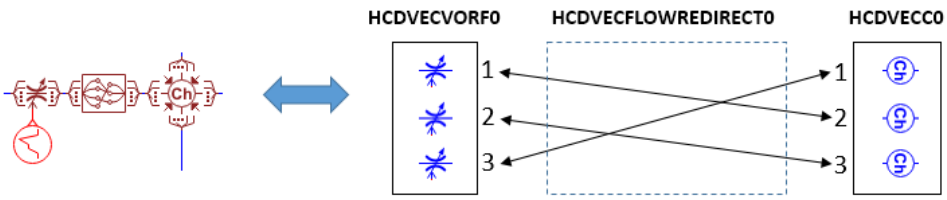

Figure 27: Graphic representation of redistribution between chambers

Simpler, however, is the "vecvarorif" module because in the case study there is no condition of variability as a function of the angle; therefore, it can be assimilated to a simple orifice with a rectangular and constant section of dimensions equal to the entire circumference, height equal to the clearance between stator and external rotor.

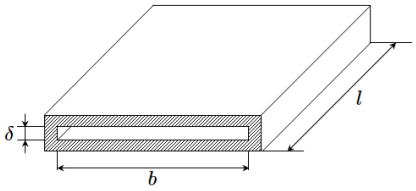

Figure 28: Equivalent representation of rectangular orifice

Unlike the gerotor, the vane pump has interactions between the various parts of more complex simulation. The pump is composed as follows: the rotor is fixed to the rotating shaft; on the rotor there are the housings for the blades, which being dragged of the rotor in motion; To contain blades there is the stator that in an eccentric position with respect to the rotation shaft compresses or releases the paddles. To ensure fluid tightness and avoid leaks between chambers, the blades are pressed against the inner surface of the stator by the springs inside the rotor. To ensure the displacement values previously set Vp = 100 [cc/rev], refers to the geometric values in Table 10.

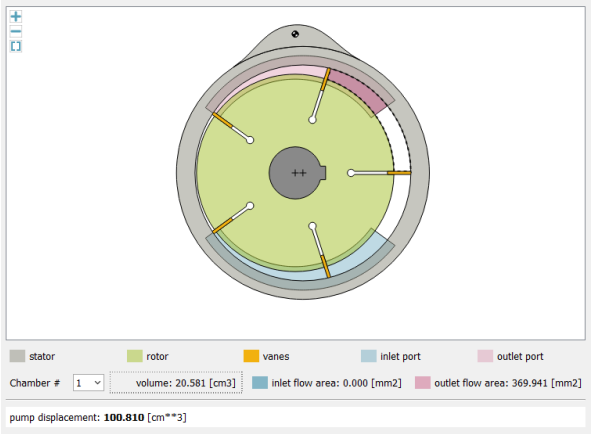

Figure 29: Vane pump profile

Number of vanes	5	-
Vane thickness	2	mm
Radius of vane tip	3	mm
External diameter of the rotor	128	mm
Internal diameter of the stator	140	mm
Vane width in axial direction (H)	25	mm
Pivot abscissa	0	mm
Pivot ordinate	90	mm
Initial stator abscissa	5	mm
Initial stator ordinate	0	mm

Table 10: Vane pump model parameters

As easy to imagine, the structure of the vane pump is more articulated, because in addition to having to size the main module in which all the geometric values are contained, Additional modules are needed to simulate the interactions more accurately between the parts, for example between blades and stator. For this purpose, the "pivoting_fric" module is used, which facilitates the study of internal, external leakages and blade friction against the stator, as shown in Figure 30.

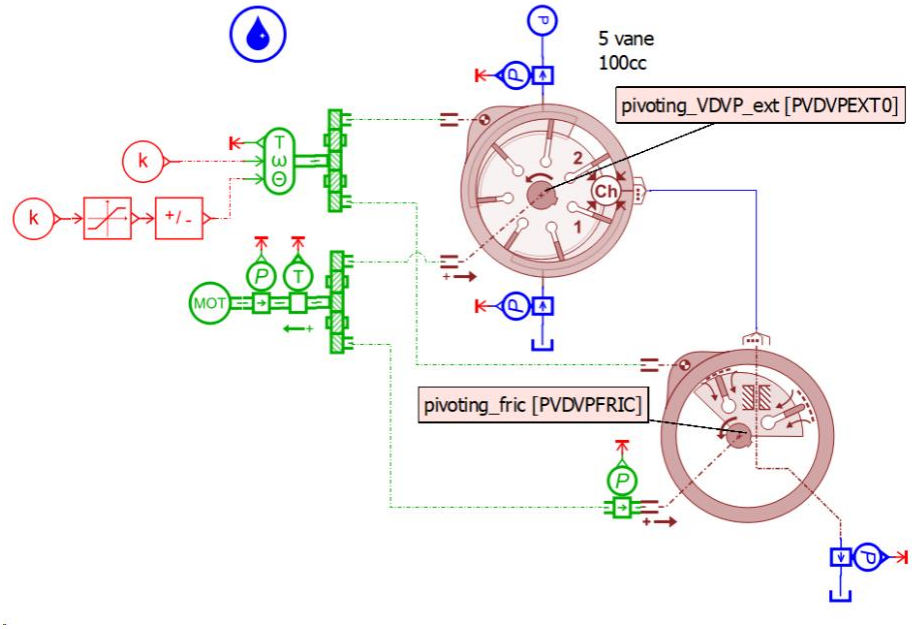

Figure 30: Complex Vane pump leakages and friction model

It was chosen to adopt exactly five "vane" because from the experimental values it was shown as an odd number present less irregularities of flow than even number "vane". A further comparison was made comparing five and seven "vane", the result showed that with a greater number of sectors increases the power dissipated without significantly improving the leakages or the regularity of the flow.

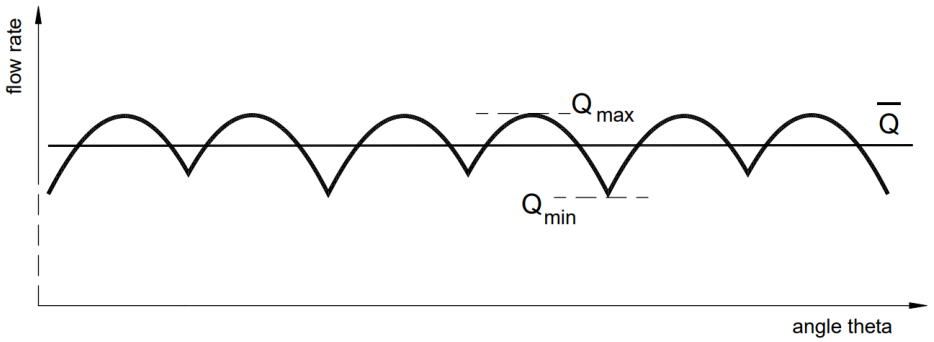

Figure 31: Flow ripple representation

Equation 29:

$$\delta_Q = \frac{Q_{max} - Q_{min}}{\bar{Q}}$$

Where: δ_Q is the irregularity flow index, higher index means higher irregularities:

- Higher pressure irregularities
- Higher vibration
- Higher generated noise

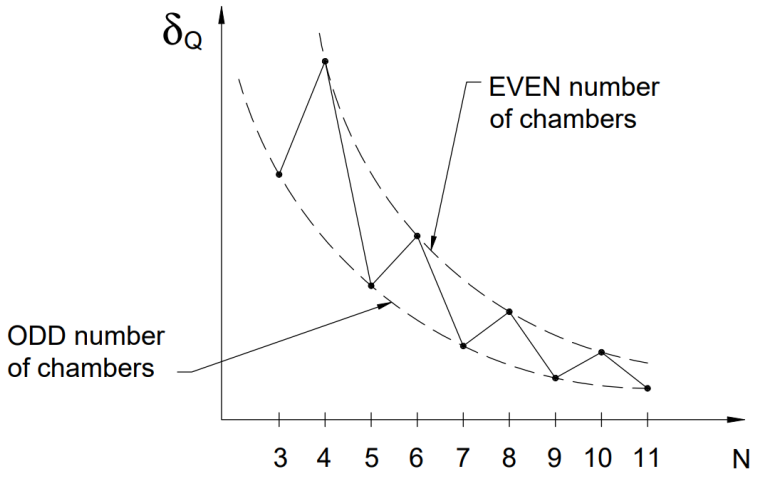

Figure 32: Odd and Even chamber effect pressure ripple index

At the same displacement, to decrease the index δ_Q:

- Increase chamber number N
- Adopt odd number of chambers

The "pivoting_fric" add-on module is able to calculate the forces exchanged between the vanes and the stator, more accurately calculating the power dissipated by friction. In addition, it is possible to estimate internal and external leakages by entering the values of the clearance between the parts. The internal leakages between the chambers caused by the clearance between the side of the blades and stator or by the non-adhesion of the "head" of the blades against the stator. External leaks are to be considered those flows that pass from the chambers outwards, through the clearance between the outer ring of the rotor and the stator or between the blades and the housing of that.

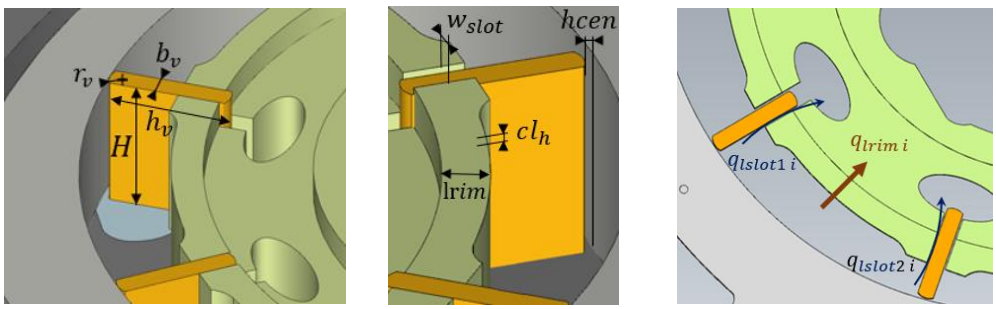

Figure 33: Representation of dimensions of pivoting_friction module

In addition, the viscous friction of the fluid that is dragged from the outer ring of the rotor against the stator is also calculated. the friction is inversely proportional to the external leakage through the ring, as the increase of the ring increases the resistance to drawing but also increases the surface of viscous friction.

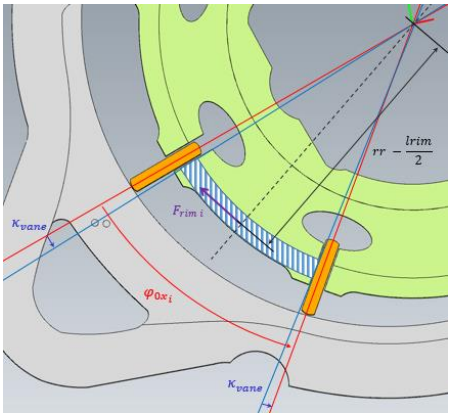

Figure 34: Representation of viscous Rotor ring friction

Following are values of module “pivoting_friction”:

Number of vanes	z	5	-
External diameter of the rotor	Dr	128	mm
Internal diameter of the stator	Ds	140	mm
Pivot abscissa	-	0	mm
Pivot ordinate	-	90	mm
Initial stator abscissa	-	5	mm
Initial stator ordinate	-	0	mm
Vane thickness	bv	2	mm
Vane tip radius	rv	3	mm
Vane width in axial direction	H	25	mm
Vane height	hv	25	mm
Clearance between rotor rim end housing (one side)	clh	0,02	mm
Rotor rim radial length	lrim	10	mm
Rotor slot width	wslot	2,2	mm

Table 11: Data of Pivoting_friction module

The transposition of both models so detailed makes the overall simulation of the system quite heavy and time-consuming. For this reason, it was decided to collect data under specific boundary conditions, with the aim of an equivalent transposition that reflects the data collected.

Then, an equivalent model of the system was regenerated with the adoption of equivalent orifices for the generation of previously simulated hydraulic losses, in addition to a correction of volumetric and mechanical returns. To simulate the internal friction of the pump, a linearly proportional resistance power was applied to the rotation speed of the pump. The result becomes an approximation, but sufficiently accurate for the purpose. The orifices now have an equivalent section simulating the external leakages, having the same flow rate as those obtained with the "pivoting_friction module”.

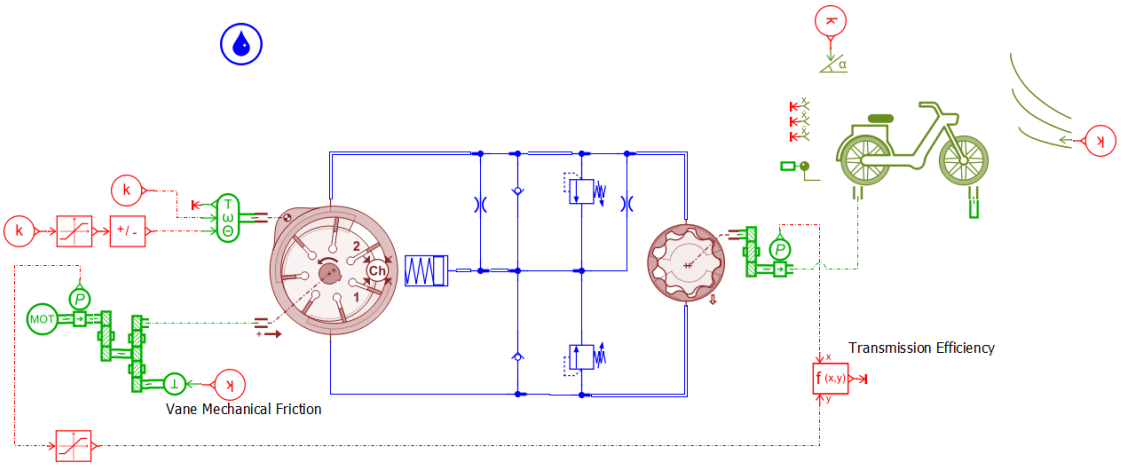

Figure 35: Complete scheme of hydraulic transmission

Given the good level of simulation complexity, a module has been added for the calculation of transmission efficiency, the purpose is to compare the system with a traditional chain transmission. Taking the torque and the speed to the pedals and the wheel, is possible to calculate the difference in power at input and power used, the greater the energy lost, the lower the performance of the transmission.

With the current model it has been tested the achievement of the speed in four slope conditions, whatever the slope is maintained the same efficiency trend, that is to achieve the efficiency between 0,6 and 0,7. The result does not promise to improve significantly, however it is in line with expectations. Image 36 shows the transmission performance that reaches the stationary state only just before the five seconds of the simulation. Since the transmission efficiency is calculated as the output power divided by the input power to the transmission, it means that during the transition phases where the efficiency is zero, the output power is also zero, because the system accumulates energy and only upon achieving internal energy balance, the transmission is able to transfer to the wheel a percentage of the input power.

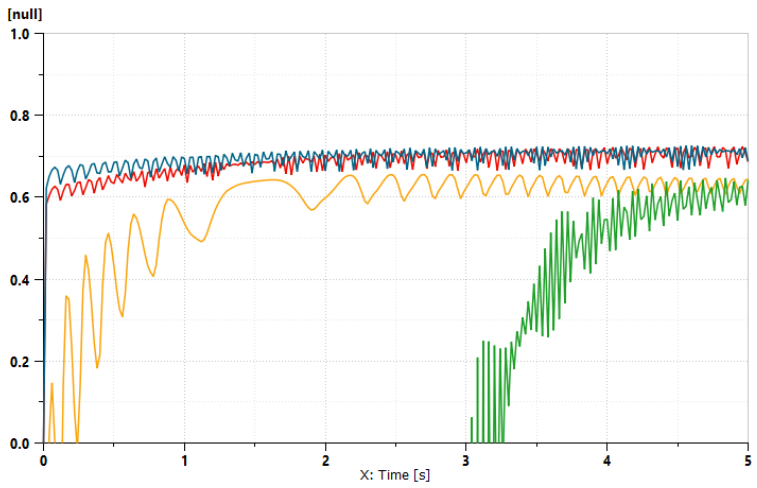

Figure 36: Efficiency of transmission which pass from transient to stationary condition

3.2.3 Displacement variation

Subsequently, all those conditions of normal use, previously omitted, are considered. For example, the intermediate displacement pump will be used during the flat pedaling condition and at low speed, only in conditions of high slope or high speed will the maximum displacement pump configuration be used. In this configuration the only variable on which you have control is the displacement, if you consider the power provided as at maximum potential.

In order to fine-tune the pump, the available power is calculated as a function of speed. To find a power curve generated by a cyclist, reference is made to specific texts such as the Allen H & Coggan AR, 2006 statistical collection, summarized in image 37. Which groups cyclists with different training history and classifies them according to their power weight ratio. For a cyclist belonging to the category of the "untrained", there are values corresponding to a request for a continuous average power of one minute.

Maximal power output (in W/kg)

	Men				Women			
	5 s	1 min	5 min	FT	5 s	1 min	5 min	FT
World class (e.g., international pro)	24.04	11.50	7.60	6.40	19.42	9.29	6.61	5.69
	23.77	11.39	7.50	6.31	19.20	9.20	6.52	5.61
	23.50	11.27	7.39	6.22	18.99	9.11	6.42	5.53
	23.22	11.16	7.29	6.13	18.77	9.02	6.33	5.44
	22.95	11.04	7.19	6.04	18.56	8.93	6.24	5.36
	22.68	10.93	7.08	5.96	18.34	8.84	6.15	5.28
	22.41	10.81	6.98	5.87	18.13	8.75	6.05	5.20
Exceptional (e.g., domestic pro)	22.14	10.70	6.88	5.78	17.91	8.66	5.96	5.12
	21.86	10.58	6.77	5.69	17.70	8.56	5.87	5.03
	21.59	10.47	6.67	5.60	17.48	8.47	5.78	4.95
	21.32	10.35	6.57	5.51	17.26	8.38	5.68	4.87
	21.05	10.24	6.46	5.42	17.05	8.29	5.59	4.79
	20.78	10.12	6.36	5.33	16.83	8.20	5.50	4.70
	20.51	10.01	6.26	5.24	16.62	8.11	5.41	4.62
	20.23	9.89	6.15	5.15	16.40	8.02	5.31	4.54
Fair (e.g., cat. 5)	13.98	7.25	3.77	3.11	11.45	5.94	3.19	2.65
	13.71	7.13	3.67	3.02	11.23	5.85	3.09	2.57
	13.44	7.02	3.57	2.93	11.01	5.76	3.00	2.49
	13.16	6.90	3.46	2.84	10.80	5.66	2.91	2.40
	12.89	6.79	3.36	2.75	10.58	5.57	2.82	2.32
	12.62	6.67	3.26	2.66	10.37	5.48	2.72	2.24
	12.35	6.56	3.15	2.58	10.15	5.39	2.63	2.16
Untrained (e.g., non-racer)	12.08	6.44	3.05	2.49	9.94	5.30	2.54	2.08
	11.80	6.33	2.95	2.40	9.72	5.21	2.45	1.99
	11.53	6.21	2.84	2.31	9.51	5.12	2.35	1.91
	11.26	6.10	2.74	2.22	9.29	5.03	2.26	1.83
	10.99	5.99	2.64	2.13	9.07	4.94	2.17	1.75
	10.72	5.87	2.53	2.04	8.86	4.85	2.07	1.67
	10.44	5.76	2.43	1.95	8.64	4.76	1.98	1.58
	10.17	5.64	2.33	1.86	8.43	4.67	1.89	1.50

Figure 37: Benchmarks for the Power Profile test by Allen & Coggan (Allen H & Coggan AR, 2006).

From now on the total mass of the system will be assumed to be 100 [kg], that is the sum of the mass of the cyclist 80 [kg] and the mass of the bicycle with the hydraulic system included 20 [kg].

Calculating that a man cyclist of 80 [kg] mass has no training experience will have a Power/Weight ratio$K_{p/m} = 6\ [W/kg]$. With which it is possible to theoretically calculate its maximum available power for non-continuous high load requests:

Equation 30:

$$P_{max,teo}\,[W] = m\,[kg] * K_{p/m}\left[\frac{W}{kg}\right] = 80 * 6 = 480\,[W]$$

The pedaling has a characteristic power curve: at zero rotation speed and at maximum speed you have zero power; there is the peak power, instead, at intermediate speed. The power curve was calculated considering the maximum torque T_{max} = 120 [Nm] and the maximum rotational speed n_{max} = 150 [RPM]; the two entities were considered linear and inversely proportional to each other, it has been shown that a non-professional cyclist tends to lose coordination at high rotational speeds, thus reducing pedal thrust. For good approximation we get the power curve below the image 38.

Equation 31:

$$P_{max}\,[W] = T_{max}\,[Nm] * n_{max}\,[rpm] * \frac{2 * \pi}{60}$$

Maximum Available Power @75rpm	471	W

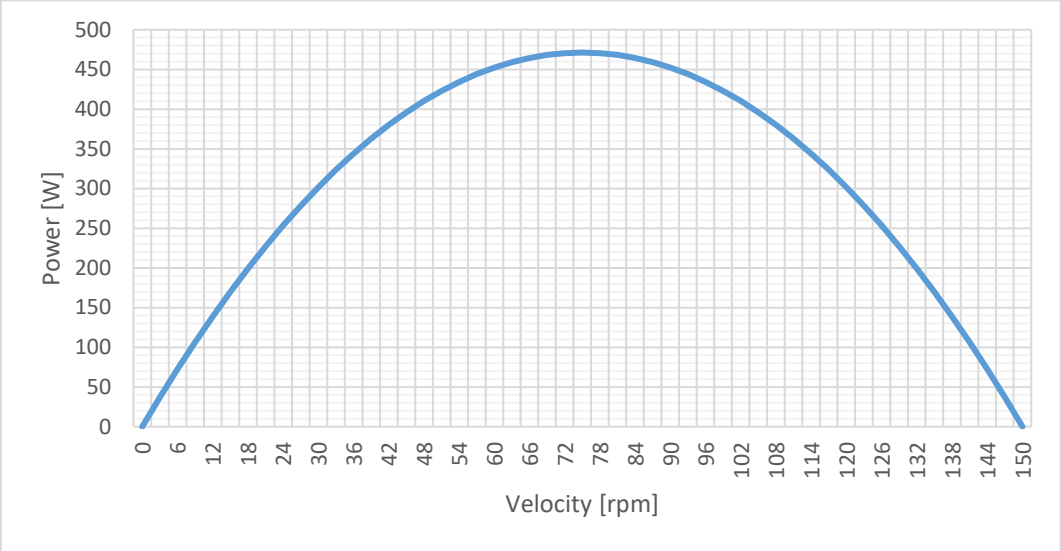

Figure 38: Theoretical non-professional cyclist power curve

Now that we have obtained the theoretical curve of a probable cyclist, we want to find the ideal gear ratio to optimize the use of the transmission and make the cyclist work in the most favourable condition at the given boundary condition.

The first point concerns the study of the transmission at the variation of displacement and pedaling speed. To obtain the different displacements of the pump it was decided to use the maximum displacement of the pump $V_{max} = 100\,[\frac{cc}{rev}]$ and to gradually reduce it with regular intervals until the value of $V_{min} = 60\,[\frac{cc}{rev}]$, then reaching 60% of its initial displacement. This range was divided by ten, obtaining eleven equispaced displacements of $4\,[\frac{cc}{rev}]$. The rotational speeds shall include eight rotational speeds between $30\,[rpm]$ and $100\,[rpm]$ with intermediate step of $10\,[rpm]$. Another condition that we wanted to insert is the slope, which

has been kept at zero to not include in the simulation energy absorption phenomena attributable to characteristics of the test environment.

The goal is to collect data from the Amesim model by simulating different combinations of variables such as pedaling speed and displacement, to search for and select suitable combinations in order to obtain the power curve to be followed by the transmission control system. The data sought correspond to the power and speed of the vehicle when the stationary conditions are reached. Before steady-state conditions, the simulation data are not representative as they are subject to transitory and non-repeatable phases. As an additional control of the simulation, the pressures of the accumulation system were checked to verify that the system never stalled during the simulations.

The power and speed data generated are enclosed in two dedicated matrices, in which for each combination of pedaling speed and displacement corresponds to a unique value of power employed or speed reached. In the figure 39 the representation of the powers grouped by rotation regime.

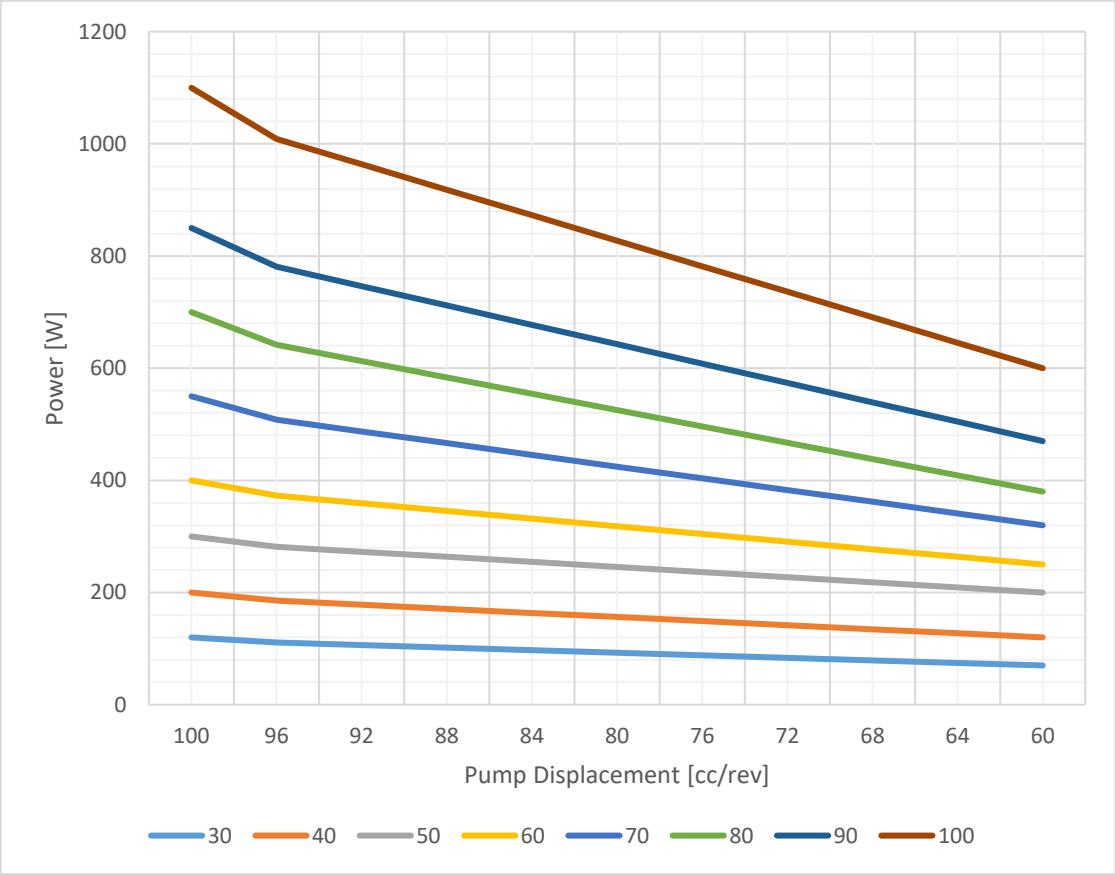

Figure 39: Power matrix representation

Subsequently, the most favourable conditions from the matrix were chosen manually, choosing those displacements that could allow a gradual growth of the necessary power and consequently ensure a linear progression during the change in displacement. In the specific case, the choice has led to the displacement between $V = 100\ [\frac{cc}{rev}]$ and $V = 72\ [\frac{cc}{rev}]$. The power data contained in the matrix represents the power required for the motion.

As already shown in the curve in image 38, the maximum available power is fixed around 75 [rpm], with its progressive reduction away from the ideal speed. The aim of the system is to keep the pedaling speed as close to the optimum speed as possible by maximising the available power.

The speed matrix of the vehicle at full speed, shown in Table 12 below, was used to verify that the displacements chosen could actually satisfy a use of the transmission on a bicycle. In this configuration, with the powers allowed by the cyclist you can travel at a maximum speed of about 30 [km/h], more than enough in the city.

Speed [km/h] / V [cc/rev] / Rotation speed [rpm]	100	96	92	88	84	80	76	72	68	64	60
30	12,0	11,5	11,0	10,5	10,0	9,5	9,0	8,5	8,0	7,5	7,0
40	16,4	15,7	15,0	14,3	13,6	12,8	12,2	11,5	10,8	10,2	9,5
50	20,7	19,9	19,0	18,0	17,2	16,4	15,5	14,7	13,8	13,0	12,0
60	25,0	24,0	23,0	21,9	20,9	19,9	18,9	17,8	16,8	15,8	14,8
70	29,2	28,1	27,0	25,8	24,5	23,2	22,0	20,9	19,7	18,3	17,1
80	33,8	32,3	31,0	29,6	28,0	26,9	25,2	24,0	22,6	21,0	19,8
90	38,0	36,5	35,0	33,4	31,8	30,1	28,6	27,0	25,5	24,0	22,3
100	42,4	40,8	39,0	37,2	35,2	33,7	31,9	30,1	28,3	26,8	25,0

Table 12: Speed matrix

Putting in relation the curve of power demand and available power to the pedals identifies the critical point of operation, in the intersection, that is the point beyond which the rider will not be able to go because it must provide a power greater than his maximum power, its point of maximum travel speed and maximum pedaling speed. To avoid reaching the maximum available power is possible to choose an underspeed approach, which means to choose a "shorter" ratio sacrificing the maximum speed achievable, but allowing to reach a lower torque to the pedals at the expense of increased pedaling speed. In the "underspeed" configuration the displacement is between 85 and 56 [cc/rev], in the graph in figure 40 the power curves just described are represented.

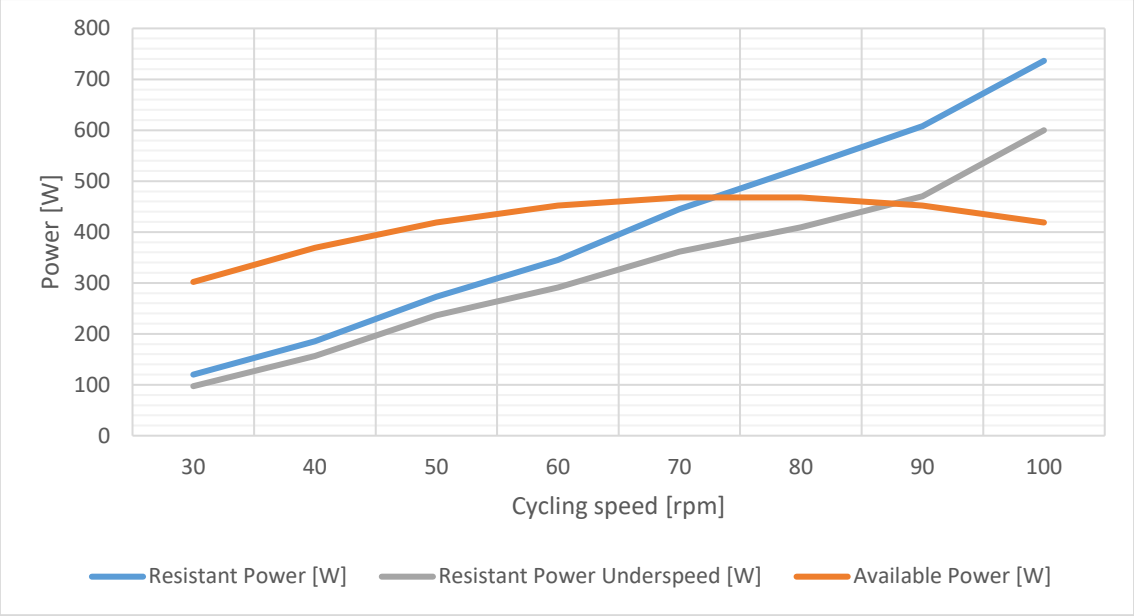

Figure 40: Available and Resistant power

The two control profiles have different speed profiles, as well as power curves. The standard profile prefers torques to larger pedals and lower rotational speeds, the "underspeed" configuration allows the reverse trend. The speed and displacement of the pump are shown in the graph in figure 41, in which are also shown the displacements selected for each speed.

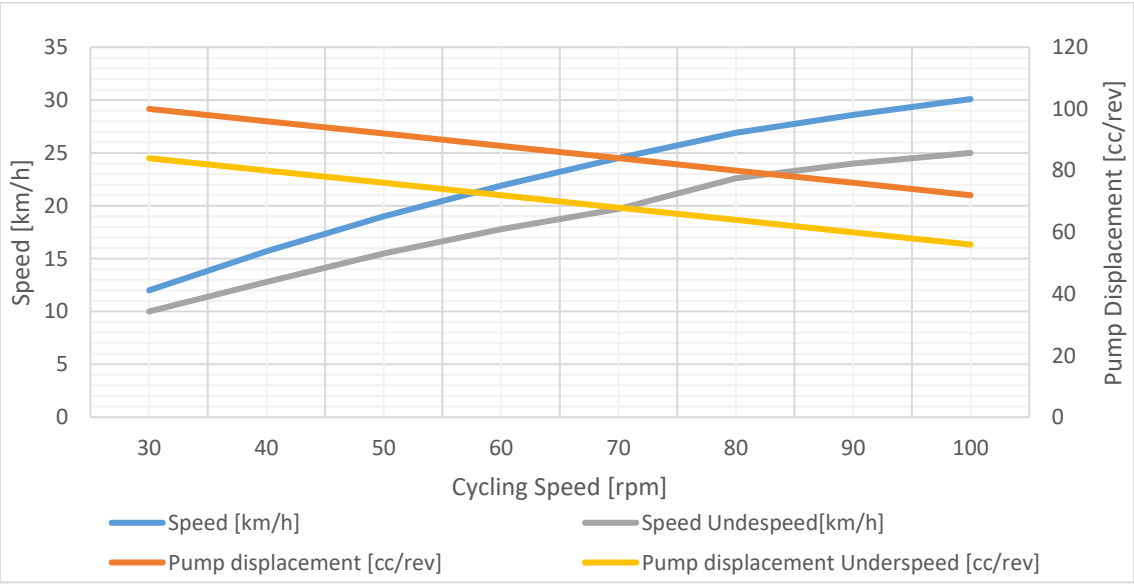

Figure 41: Speed and Pump displacement behaviour during transmission regulation

During these numerous simulations, information on the performance of the transmission in constant-speed phases was also extrapolated, as for the power input and speed data. Regardless

of the conditions of use, the overall returns remain low, always below 60% and unmistakable with a traditional bicycle chain, which has significantly higher efficiency. At this point in the analysis, therefore, the solution to the commercial implementation of the system is considered a failure.

Trans. Efficiency [-] V [cc/rev] / Rotation speed [rpm]	100	96	92	88	84	80	76	72	68	64	60
30	0,58	0,55	0,53	0,52	0,50	0,49	0,47	0,46	0,44	0,43	0,41
40	0,56	0,53	0,52	0,50	0,49	0,47	0,46	0,44	0,43	0,41	0,40
50	0,57	0,54	0,53	0,51	0,50	0,48	0,47	0,45	0,44	0,42	0,41
60	0,50	0,48	0,47	0,46	0,45	0,43	0,42	0,41	0,40	0,39	0,38
70	0,48	0,46	0,46	0,45	0,44	0,43	0,42	0,41	0,41	0,40	0,39
80	0,45	0,44	0,43	0,42	0,41	0,41	0,40	0,39	0,38	0,38	0,37
90	0,42	0,41	0,40	0,39	0,39	0,38	0,38	0,37	0,36	0,36	0,35
100	0,42	0,41	0,40	0,40	0,39	0,39	0,38	0,38	0,37	0,37	0,36

Table 13: Transmission efficiency matrix

3.2.4 Considerations

Pursuing the desire to adopt a hydraulic transmission could collect points in favour of and against its adoption on a vehicle of the bicycle category.

Among the pros there are definitely:

- Continuous variable ratio transmission
- Maintenance on the hydraulic machines is low
- Flexibility in customizing the adjustment profile by varying the range of the pump displacement

While among the cons:

- Overall low transmission efficiency

The very low efficiency makes the product difficult to imagine on the market, because they require the cyclist to use at least twice the power in most of the conditions tested. The highest efficiency value was found at high loads (cylinder capacity of 100 [cc/rev]) and low pedaling speeds (30 [rpm]). The study wants to pursue on a possible application also experiencing deep changes in its structure, because the advantages that have been found by simulations are of interesting application.

4. Changes on project

Variations have been studied to compensate for the most serious problems, such as the very complex regulation system and the reduced efficiency.

First step taken to partially compensate for the displacement adjustment: a pilot line has been developed based on the automotive circuit, in order to improve the reliability of the system while maintaining its positive characteristics.

Subsequently, it was decided to follow a different line of development, separating from the original idea and adopting a deep change of the project. A new hydraulic system has been developed and studied to improve energy efficiency in a cycle of use of a bicycle, experimenting with a kinetic energy recovery circuit in the braking phases, to be placed in parallel with a traditional chain transmission.

4.1 Automotive control system replacing the centrifugal control system

The regulation system controlled by the centrifugal force is very complex and difficult to implement, considering that the high number of components could give symptoms of low reliability over time. Was decided to vary the design to develop a control system of a different nature and that can be more adaptable to the needs of the cyclist.

The solution will not lead to an improvement in the overall efficiency of the transmission, but simply a better controller and reliable displacement adjustment.

In heavy-duty vehicles, a hydraulic circuit called "automotive control" is used to regulate a hydraulic transmission. The system consists in the use of a small and fixed displacement pump mounted parallel to the main pump, which will generate a flow linearly dependent on the rotation speed of the main pump, but the flow is fed into a pilot circuit. The pressure that will be generated on the line will be in relation to the flow and the calibrated hole at the exit; doing this, at constant section of the hole, the pressure will be in function of the pump speed rotation. The pressure and the flow will be sufficient for the actuation of the linear actuator for the regulation of the displacement of the primary pump, the greater the pressure on the pilot line, the greater will be the displacement regulation, then the greater will be the displacement. Because if the higher the pedaling speed, the lower the torque exerted by the cyclist; to restore the optimal pedaling speed and rise the available power will be rise of the displacement, which will increase the resistance at pedals and then the cyclist will decrease the pedaling speed, reaching the balance dictated by the cadence of pedaling.

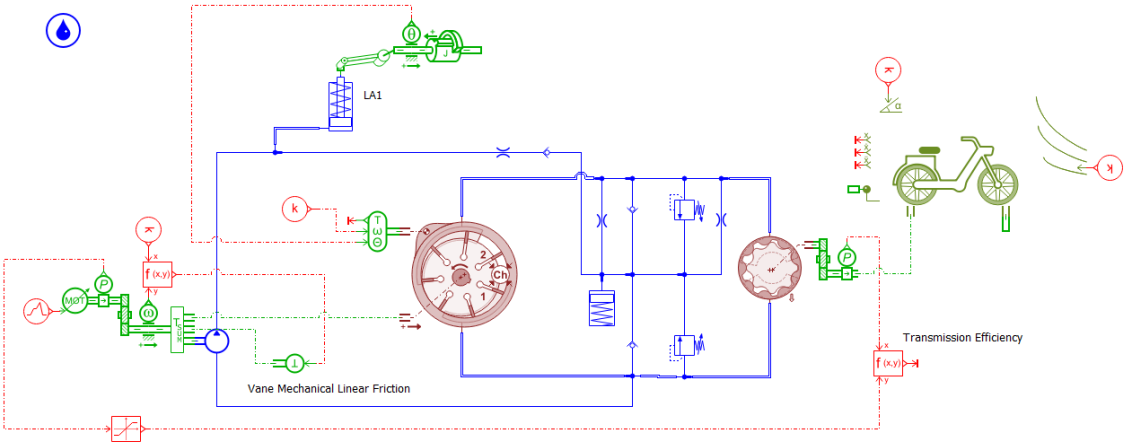

Figure 42: Automotive control with one actuator

Note that the pilot circuit is discharged onto the internal line to minimize pressure influence, the point where the lowest and most constant pressure of the circuit is obtained. Moreover, the flow rates are extremely low, so even the power dissipated by the auxiliary pump will be minimal. If the pilot line were discharged on the high line, the dissipated powers would be greater, because the minimum pressures will be equivalent to the high transmission pressures of the motion. If, instead, the pilot flow was to be discharged on the low line, the circuit would have a flow that would discharge directly to the sampling point rendering null the contribution of the secondary pump. Among the benefits of discharging on the internal line is the possibility of ensuring a constant flow to the accumulator, which will always have a positive minimum pressure available to avoid discharging completely and at the same time to ensure it even in the low line.

The dimensions of LA1 actuator for which operating equilibrium has been achieved are:

D_{LA1}	25	mm
S_{LA1}	6	mm
k_{LA1}	3	N/mm
$F_{Pre,LA1}$	40	N

Table 14: LA1 actuator geometry dimensions

Which corresponds to: D_{LA1} Actuator diameter, S_{LA1} Actuator stroke, k_{LA1} Spring elastic constant and $F_{Pre,LA1}$ Spring preload.

The actuator so dimensioned will have a working range between 0,81 and 1,18 [bar], the very low saturation pressure will reduce the power dissipated on the pilot line. The saturation pressure means to be that pressure beyond which the displacement is no longer regulated because the actuator is placed at the end of the stroke, that is, the upper pressure limit.

The operating pressures vary depending on the calibrated hole chosen to be adopted, each cyclist may have their own preference; then choose whether to take in action before or after the adjustment, shifting or widening the range of the pressures obtained by the pedaling speed.

The layout just shown is very simplified in its composition and operation. The regulation takes place only as a function of the pressure that is generated in the pilot line, this means that the system is affected by the lower pump rotation speed and therefore by the pedaling speed. The faster the pedaling, more the LA1 actuator will increase the displacement of the primary pump, increasing its flow and therefore at a higher speed of the vehicle, on counterpart generating a greater torque to the pedals. It has limits of versatility, but is very simple and achievable with relatively inexpensive components. The actuation principle is almost the same as the regulation implemented by the centrifugal force, with the advantage of having an easy adjustment.

Like the previous method of adjustment, the system begins to present the first deficiencies when changing the torque resistant to the higher displacement, for example in climb condition. The motor would require a higher pressure, therefore the pump should reduce the displacement to allow to reduce the driving torque, but this would not happen because the regulation system is insensitive to the pressure in the main line. At the same time, it would be counterproductive to have the pilot line unloaded on the high line, because the automotive control would record a greater pressure increasing proportionally the displacement, further increasing the torque to the pedals. The ideal condition would be to have a system that simultaneously can track the change in cadence and pressure on the main line, to be able to increase the displacement as the cadence increases and to decrease the displacement as the inlet pressure to the displacement increases. With the current layout the adjustment is not possible, so please refer to the next paragraph in which you have simulated the most complete automotive control.

4.1.1 Optimal displacement analysis and LA2 addition

The aim of the system is to keep as high as possible the level of comfort perceived by the cyclist during slopes and speeds vary. Up to now the displacement has changed according to the speed of travel; to make the system more complete it was decided to insert an additional actuator, which will adjust the displacement of the pump according to the power required.

In hill conditions, more torque is required on the wheel, which requires more pressure on the high line, requiring more torque to the pedals from the cyclist. The "automotive control" includes a version with an additional actuator, in this case it will be called LA2.

Before continuing, we want here to define the concept of "effort" that will be used from now on. For simplification of exposure will be called "effort" of the cyclist the percentage index of the maximum available power. That is, the maximum effort corresponds to the maximum power developable by the cyclist, while a comfortable pedaling condition at low effort is comparable to a low power percentage of that available. Thus, the best power ratio developed and available corresponds to the pedaling speed of about 75 [rpm], because it is located at the maximum power available. In conditions of constant resistant power, a lower percentage value of effort is obtained if the rider proceeds at optimal pedaling speed. So, to pursue the goal of maximum pedaling comfort you want to ensure that you keep the effort minimal, although this will include the use of more power by the cyclist, because even if the power value rises it is possible that the cyclist feels less fatigue since he is in better conditions and with lower percentage levels of effort.

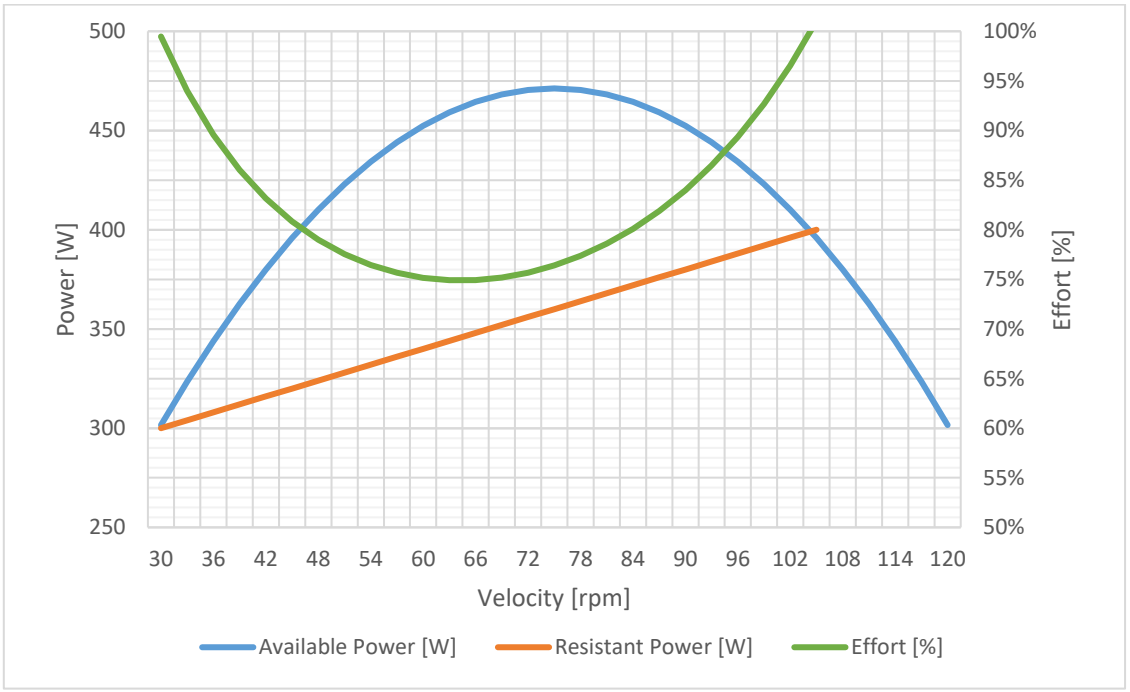

Figure 43: Effort behaviour on linearly constant required power increase

The effort trend of the condition described in the example is shown, in the graph of the image 43, if the necessary power is linearly increasing as reported, the minimum effort condition will

be reached at the speed of 65 [rpm] in how many you have great availability of power, but at the same time a low demand by the system.

Continuing now the description of the new system layout with auto control; to reduce the effort of the cyclist is needed to insert the actuator LA2 for the adjustment of the displacement as a function of the load. The second actuator this time placed on the main line at high pressure, as in the diagram of image 44, which will adjust the area of the variable section of calibrated hole, unlike the previous version. Now there are tools needed to track the speed of the primary pump and the pressure required by the hydraulic motor to support the motion.

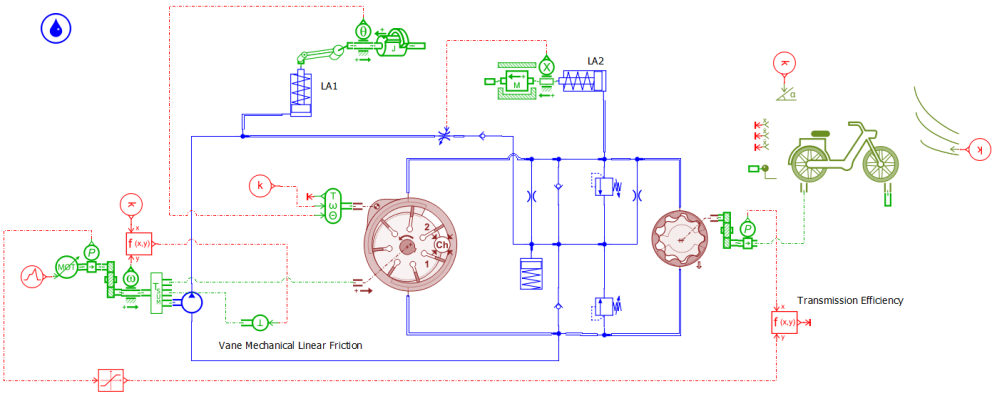

Figure 44: Automotive control with two actuators

The optimal operation foresees that with the increase of the necessary power also increases the pressure on the main line that, through LA2 will increase the area of the choke on the pilot line, which ensure to decrease the pressure in LA1, which will decrease the displacement of the main pump and therefore the flow rate; consequently, will increase the reduction factor of the transmission, increase the torque at pedals and decrease the vehicle speed. Equivalent to the use of a reduced gear of a traditional bicycle transmission.

The system, with the addition of LA2, shall be calibrated to the displacements chosen in paragraph 3.2.3. Maintaining the boundary conditions, for example the slope, the displacement and pedaling speed (therefore driving power) will correspond to a single vehicle speed, that is, the speed for which the necessary power is required. This last one shall be the power equivalent to the driving power multiplied by the efficiency coefficient of the transmission. In optimal pedaling conditions, if is changed the slope, the needed power would vary, the cyclist would have two possible choices without changing the ratio of transmission:

- Maintain the pedaling speed, therefore also the vehicle speed, increasing the power required to the pedals and consequently also the effort.
- Decrease the pedaling speed, maintaining the required power, but still increasing the effort, because it would move away from the optimal pedaling condition.

Both solutions have a greater percentage of effort than the original condition, this is because, as already explained, moving away from the optimal regime even keeping the power unchanged, the rider will be forced to use a greater percentage of its available power defined as "effort”.

The configuration allows to maintain high pedaling efficiency while remaining at speeds close to 70 [rpm], mitigating the increase in effort because is kept high the value of the maximum power available and consequently increasing the comfort of pedaling.

The dimensions of the LA2 actuator assumed for the simulation are:

D_{LA2}	12	mm
S_{LA2}	10	mm
k_{LA2}	6	N/mm
$F_{Pre,LA2}$	10	N

Table 15: LA2 actuator dimensions

Which corresponds to: D_{LA2} Actuator diameter, S_{LA2} Actuator stroke, k_{LA2} Spring elastic constant and $F_{Pre,LA2}$ Spring preload.

Calculating the actuator operating pressures in the range from 0,88 to 6,19 [bar], this will be the pilot pressure that will be taken from the high line for the implementation of LA2. The minimum pressure in the system is set to 0,5 [bar], then at lower speeds or with negative slopes there will be no regulation of LA2; It should be noted that the pressures reached at zero slope and steady conditions never exceed 4 [bar]. Then to get the saturation of the actuator has simulated a ride at the slope of 7°, reached this threshold of pressure will no longer be displacement adjustment, because LA2 will already be in saturation and then the calibrated hole with variable section will be completely open, on the pilot line there will be the minimum pressure and therefore the minimum displacement of the main pump.

LA2 can be defined as primary actuator and LA1 as secondary, because LA2 is independent and conditionate the actuation of LA1, but not vice versa. The dependence of one actuator for the other makes difficult the tuning of the system, described in the following paragraph.

4.1.2 Complete automotive control system set up

Automotive control system is difficult in tuning. The actuators are positioned in cascade, so the regulation of LA2 affects the regulation of LA1, chaining the effects. So, gets in advanced gradually, every time data was chosen it was wanted to simulate in Amesim the system, approaching through an iterative sequence to the final result.

The starting condition of the simulation shall be the vehicle proceeding in uniform motion at zero slope. The choice of the auxiliary pump and the pressure of the pilot line will affect the overall efficiency, because the greater the flow and pressure, the greater will be the hydraulic power that will be dissipated by the orifice. So, the choice fell on a very small displacement: $V_{P,a} = 2\ [\frac{cc}{rev}]$ to keep the flow low.

Having already sized LA1 taking into account the energy aspect, we know that the ideal operating range is between 0,81 and 1,18 [bar]. Using Bernoulli formula for turbulent regime:

Equation 32:

$$Q = C_d * A * \sqrt{\frac{2 * \Delta p}{\rho}}$$

Knowing the pump flow (Q), the fluid density and the pressure difference (Δp), it is then possible to calculate the required area to ensure that the actuator remains in the desired range. The flow is calculated starting from the pedaling speed that is wanted to preserve, which is 60 [rpm], while the pump rotates at higher speeds, thanks to the speed multiplier chosen above. By applying the inverse formula of equation 32 above we obtained the area: $A = 2{,}5\ [\ mm^2\ ]$.

Choosing this section is be ensure to reach the minimum actuation pressure from 60 [rpm] in pedaling, while at higher pedaling speed and less efficient will be the regulation of LA1. It is pointed out that the speed referred to the calculation is slightly lower than the value of 70 [rpm], in the previous paragraph indicated as optimal. The pedaling speed must be in equilibrium with the displacement adjustment; therefore, to coincide the starting speed with the ideal speed would generate a discontinuity in the adjustment, because around the operating pressures with lower values there is no regulation, while at slightly higher values the change in displacement is obtained, also if it is minimal. The adjustment discontinuity is visible from the displacement variation curve of figure 45.

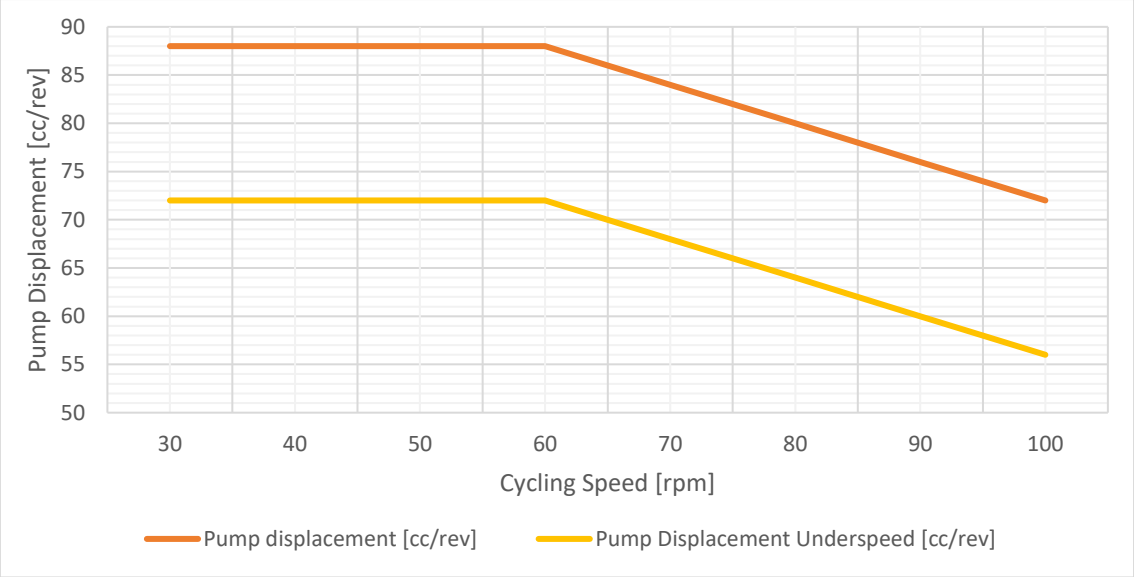

Figure 45: Pump displacement regulation

The theoretical power dissipation is calculated with the following formula:

Equation 33:

$$P_{Wasted} = Q * \Delta p$$

Where: Q is the flow rate and Δp is the pressure difference between the input and output from the calibrated hole.

During the steady-state operation simulation and with a calibrated hole with maximum section a pressure drop is recorded $\Delta p_{max} = 0{,}16\ [bar]$ and the relative flow $Q_{max} = 0{,}6\ [\frac{l}{min}]$. Under the same conditions, but with a calibrated hole with a minimum section, a pressure drop is obtained $\Delta p_{min} = 4{,}06\ [bar]$ and the relative flow $Q_{min} = 4{,}07\ [\frac{l}{min}]$. At the maximum section are calculated the power dissipated $P_{Wasted,max} = 0{,}16\ [\ W\ ]$, while at the slightest section are calculated $P_{Wasted,min} = 27{,}54\ [\ W\ ]$, in both cases the dissipated power is contained, with values up to 10% of the necessary power to the traction.

Subsequently, the normal pressures in the high line were simulated, these were the reference for relating the area of the orifice and the working pressure of LA2; in stationary conditions in the simulated model an average of 2 [bar] is calculated.

By relating the minimum regulating pressure of LA2, corresponding to 0,88 [bar], and the normal operating pressure of 2 [bar], it is obtained that the actuator in question is already in the adjustment phase. Is possible to increase the preload of LA2 to normalize the actuation, but was chosen to not take action; in the case chosen was decided for a more comfortable calibration, preferring a slightly higher pedaling speed and a lower torque at equal power. In any case, is possible to leave at the cyclist to decide how to calibrate the system according to personal preferences, precisely by intervening on the preload of LA2.

4.1.3 Considerations

The automotive control is a non-invasive and highly automated displacement control system. In contrast to the adjustment by means of rotating masses it is highly compact, it is also less sensitive to vehicle vibration, making it a reliable solution alternative.

Advantages:

- Non-invasive, low number of components
- Good efficiency
- Reliable
- Easy personalization

Cons:

- Difficulty tuning to achieve balanced adjustment

The solution does not compensate for the efficiency problems of the hydraulic transmission, but with its version with two actuators brings into the control system the possibility of using as an input to the control logic both: vehicle speed and the torque required by the load. Two variables which apply two complementary displacement adjustment logics.

4.2 Project reinterpretation for efficiency performance improvement on riding cycle and hydraulic accumulation

The hydraulic transmission brings with it some disadvantages of energy dissipation due to its nature, which lead to not prefer this type of solution in the application of such a small circuit; despite the great versatility that could be obtained, in a vehicle like the bicycle is not fully exploited.

It was decided to find an alternative that would match the advantages of a hydraulic circuit with the simplicity and efficiency of the bicycle chain transmission. Focusing on the desire to achieve an improvement in pedaling comfort by exploiting the ease of energy conversion of a hydraulic circuit, was decided to get an accessorial circuit to the traditional chain transmission, with the implementation of an accumulator, which will convert the kinetic energy of the vehicle into hydraulic energy. That is a hydraulic system capable of recovering the energy of the vehicle while braking, making it available at the restart, called with the acronym of KERS (Kinetic Energy Recovery System) in its most general conception. Ideally, the reference scheme is the one shown in image 46, which will be adapted to the nature of the vehicle here in the studio.

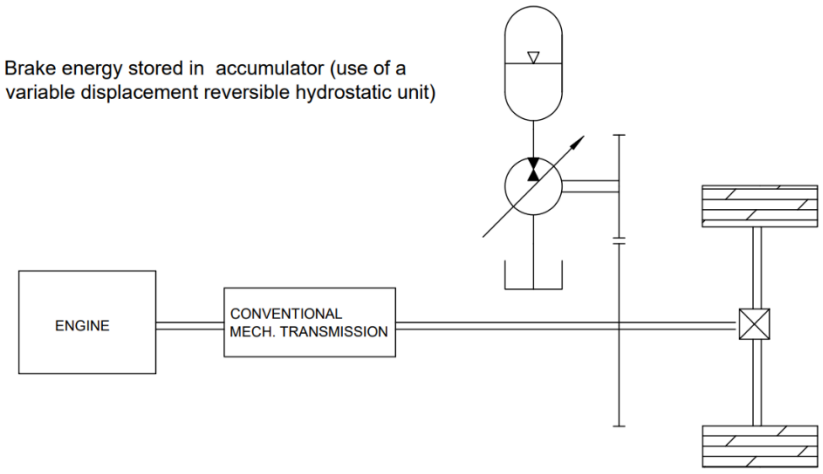

Figure 46: Engine Vehicle Hydraulic KERS

With this ideal line of development, it is expected to realize a hybrid transmission, with which it will have minimal energy losses in stationary conditions, but intervening on the braking system will accumulate the energy necessary for braking, that can be used to support the restart depending on the rider's command. The system will potentially use a smaller displacement hydraulic machine.

4.2.1 State of the art

The hydraulic KERS is used on some heavier vehicles given the great powers available, allowing considerable advantages in terms of wear of the components in braking and energy saved at the restart. The system includes a few components: a hydraulic machine connected to the transmission of the vehicle, able to operate as a motor and as a pump; a valve pack to manage the directionality of flows to and from the motor or pump; Finally, the two accumulators, one at high pressure for the accumulation of oil under pressure and one at ambient pressure for the reserve oil not under pressure. Figure 47 shows the flow direction during the two main phases of operation, namely regeneration (braking) and release (acceleration).

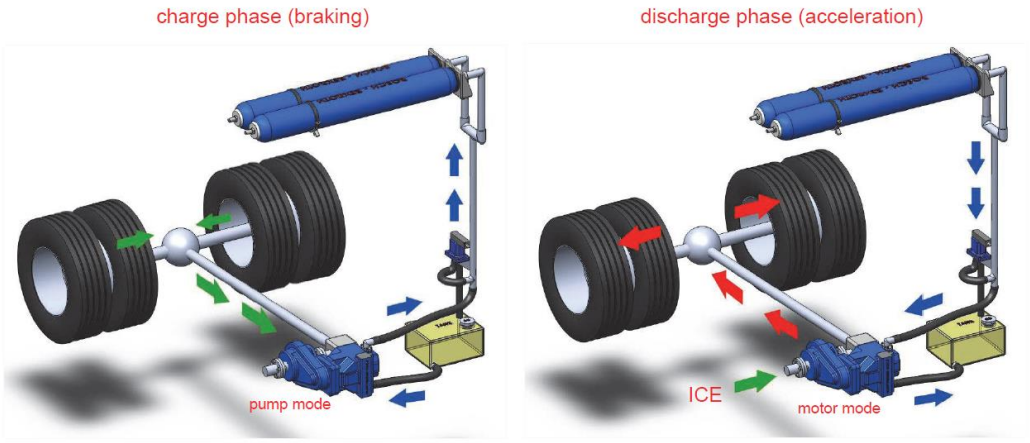

Figure 47: Heavy duty vehicle Hydraulic KERS

For bicycles has been designed and put on the market an electronic accumulation system of equivalent operation. This has a wheel hub comprising everything needed: accumulation batteries, enough to accumulate energy for some phase of acceleration; the power electronics, to convert current and voltage by interfacing battery and motor (or generator) as needed; the control electronics, to manage the logic of operation and interface with the cyclist; and finally, the motor/generator.

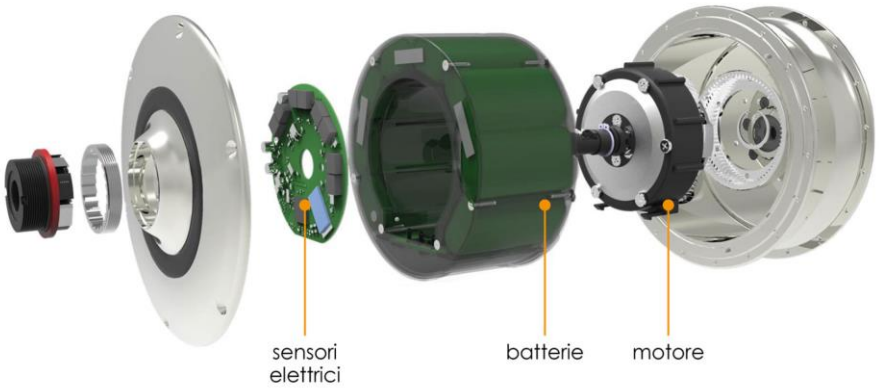

Figure 48: ZEHUS bike hub system components

The system activates the braking with the counter-pedaling movement, that is the movement of the pedals in reverse rotation, is able to return the energy with two principles of use: constant automatic aid with maintenance of the charge, or with a remote button on the handlebar until the release of the command. The first consists in the minimum use of energy to assist the cyclist as much as possible during the ride, the second principle is simply based on the direct command of the cyclist. Of course, this system, like the hydraulic one shown above, does not require external energy supplies for the recharge of the accumulator, because it is able to accommodate the braking and acceleration phases to optimize the energy flow; The two systems have the only scope of making the journey from point "A" to point "B" more efficient and do not have the scope of assisting the ride with an external supply of energy, as so many available on the market today.

The electronic storage system for bicycles shown is very interesting because it is flexible and adaptable to many conditions of use, unfortunately it remains limited by batteries and power electronics. The batteries, however functional and compact, are subject to wear, aging and have an intrinsic value economically high given by the noble materials used, unattractive to those who would make an occasional use; while the power electronics is limited by managing powers, as these systems are generally designed to handle peak and nominal power according to their size, during the conversion of the current have a tendency to overheating by effectively limiting their operation, sometimes insufficient in the stress conditions and sometimes oversized for the nominal load.

4.2.2 Preliminary model: divided loops and spool valve adoption

To develop the Kers hydraulic system, we proceed with the study of a preliminary model that can meet the objectives and mediates between the two solutions seen in the chapter of the state of the art. Checking step by step the effectiveness of the project with a simulation model in Amesim environment.

Conceptually are take the hydraulic storage layout for heavy vehicles and resize it to be used in a bicycle. The accumulators that are wanted to be used are spring-loaded, the choice fell on this type because they have a linear trend in function of the pressure inside the circuit, therefore potentially simple in the tuning. Unlike the heavy application, which usually uses gas accumulators, which by its nature will follow an exponential trend depending on the gas parameters. Another aspect that makes prefer the spring accumulator to other solutions is the structural simplicity, few components and easy or no maintenance needed.

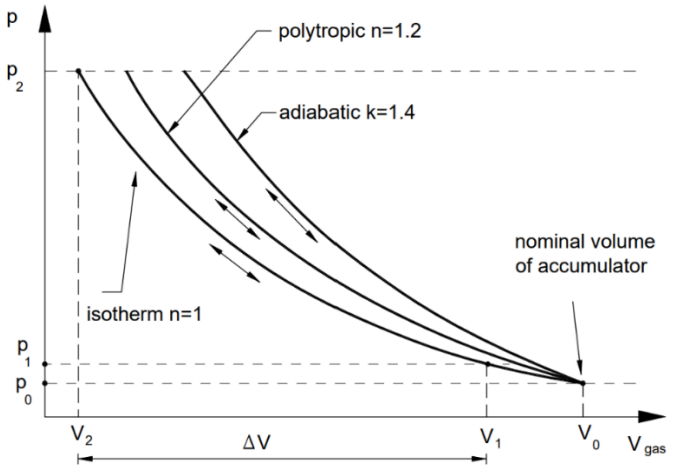

Figure 49: Polytropic behaviour of gas accumulator

The accumulation system therefore has two spring accumulators, one for the storage of oil under pressure after a braking phase of the vehicle and an accumulator to contain the fluid at low pressure. Of course, the two springs, from which the properties of the accumulators are defined, are geometrically different to allow to generate different potential energy in the circuit; when the circuit has the high-pressure accumulator (HP) empty, all the fluid will be contained in the low pressure accumulator (LP) and vice versa. The circuit will have minimal potential energy when LP is loaded; instead, it will be at maximum potential energy with HP load, all this possible from the geometric balance between the two springs.

Below are the values used to size the accumulators. The preload is necessary for the definition of the minimum pressure together with the definition of the diameter (values highlighted are derived from the calculation). The maximum pressure is calculated with the product between the elastic constant and the overall preload compression and piston stroke. Attention is drawn to the values of maximum pressure LP and minimum pressure HP, this last one must be slightly higher than the first because it must not have the spontaneous motion of fluid from LP to HP without the aid of the pump. In addition, note that the volume that can accommodate LP is

slightly higher, because in the regeneration phase do not want in any case to allow the absence of fluid at the pump inlet and therefore lead to the cavitation phenomenon.

The amount of accumulable energy is low, but how possible to see from the simulations will be enough for some recovery phases. Considering that this is a pilot sizing, as it is easily development in function of the need for accumulation.

Free load	200	N
Diameter	80	mm
Area	5027	mm^2
Min Pressure	0,40	bar
Stroke	300	mm
Spring rating	12,5	N/mm
Total force	3950	N
Max Pressure	7,86	bar
Volume	1508	cm^3
Energy stored	0,156	Wh

Table 16: High pressure accumulator dimensions

Free load	100	N
Diameter	100	mm
Area	7854	mm^2
Min Pressure	0,13	bar
Stroke	200	mm
Spring rating	1	N/mm
Total force	300	N
Max Pressure	0,38	bar
Volume	1571	cm^3
Energy stored	0,006	Wh

Table 17: Low pressure accumulator dimensions

The choice of the hydraulic machine could be given on many different options: ensure more lightness rather than less leakage, or prefer higher pressures at low speeds and vice versa. In this case it was preferred to adopt for a hydraulic machine that has already been dimensioned, the gerotor, to be precise, a model already analysed in previous chapters. This should result in acceptable pressures at sufficient speeds, using a simple overall machine with a displacement of 50 [cc/rev].

The essential core of this system is the "valve body"; essential because it must optimize and ensure proper operation during all phases of use, giving higher efficiency as possible on energy side. During this first prototyping the focus will be only on its theoretical functionality, leaving out any other aspect mentioned. The circuit must take into account different conditions of use and therefore allow to change its conformation with the use of valves.

An essential simulation model has been created, that is a model able to recreate a standard virtual environment that can compare the new solutions studied with a traditional bicycle model. This will allow to understand if the new implementation schemes will have a behaviour similar to a bicycle with only human muscular traction, also to identify the phases with a potential for better efficiency.

The simulation environment shall be capable of reflecting any conditions of use that the vehicle will face. Specifically, it will have a typical pattern of standardized use specifically for the purpose:

- Starting from standstill without aids and empty system
- Maintaining the speed with empty system
- Regenerative braking to vehicle stops
- Restart with the aid of partially charged system

Other phases are not relevant because these phases are sufficient to study the behaviour of the circuit.

To differentiate the configurations was proceed by separating the circuit according to its use, the found layouts will be superimposed to create the overall circuit.

The typical conditions of use to which a specific circuit will correspond are:

- Constant pedaling
- Breaking
- Restart or acceleration

The first point refers to all those situations where there is a constant pedaling, even with small variations of slope or speed that are not tiring, even without the intervention of the hydraulic circuit. Three main solutions can be adopted to minimise flow friction at this stage.

The first is the adoption of a by-pass circuit that minimizes hydraulic losses, in the second is possible to adopt the mechanical separation of the transmission between pump and wheel, finally, the third could include a hydraulic or mechanical actuator that sets the displacement of the variable displacement pump to zero. The advantage of the by-pass is undoubtedly to be found in the layout, the fixed displacement pump remains constantly connected to the wheel, resulting in a constant dissipative loss also if it is low, but bringing constructive advantages of the transmission. The circuit in case of by-pass will simply be a closed circuit having as only element the pump and the inlet and outlet ducts connected to each other, as shown in the diagram in the image number 50.

As for the solution number two, there are great advantage of less inertia and dissipation; on the other hand, there is a more complex and a presence of mechanical disengagement, providing a clutch interposed between the wheel and the hydraulic machine.

Unlike the previous ones, the last option foresees a hydraulic machine with variable displacement, which in phases of by-pass can reduce to zero the displacement and therefore the only frictions are those of drag of the rotor.

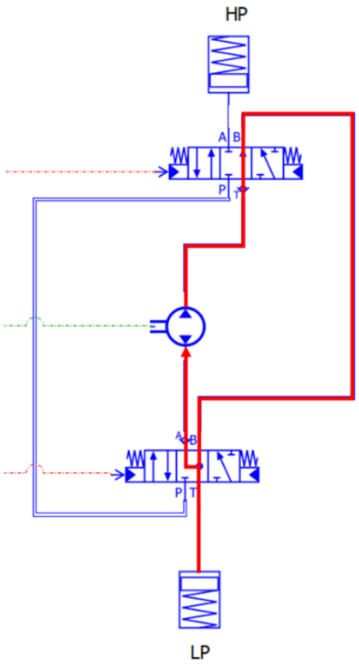

Figure 50: By-pass loop scheme

The braking phase uses the hydraulic motor to move the fluid from the low-pressure accumulator to the high-pressure accumulator, thus transforming the kinetic energy into potential energy. This energy will be firstly converted from mechanical to hydraulic, and then be converted back into mechanical energy (this time as potential) by compressing the spring in the HP accumulator. The open circuit configuration inserts the pump between the HP and LP accumulators, diagram in figure 51.

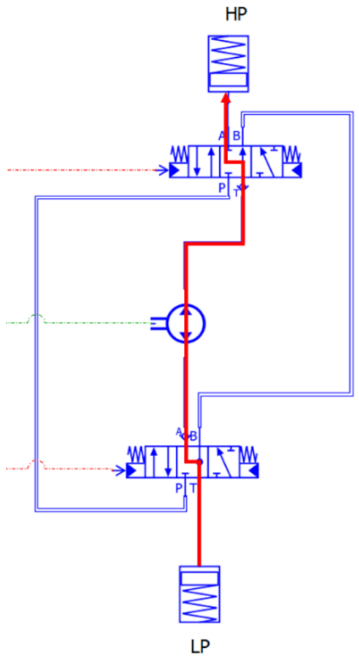

Figure 51: Regeneration/brake phase

In the scheme of figure 52 it comes analysed the last phase called release, or "boost": that is to the activation of the acceleration command, with which the energy previously stored in the accumulator HP is used in order to push the hydraulic machine now in motor configuration. This is done by making the oil flow towards the low-pressure accumulator (LP). The circuit is in open loop configuration also in this case, with the difference that lines at the input and at the output, from the motor, have been reversed with respect to the linear braking configuration. In order to avoid motion reverse by the flow reversal in the circuit, the vehicle shall not have the possibility of being driven by the motor in reverse direction.

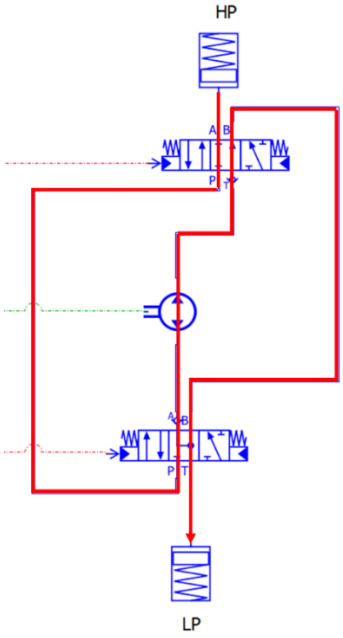

Figure 52: Boost phase

It should be noted that two separated circuits are necessary for the accumulation in braking and for the release, because the hydraulic machine will always have to rotate in the same direction of rotation; but if not, it would have a "spring" effect, which means that once accumulated potential energy in breaking it would have an equal but opposite acceleration pushing the vehicle to move to reverse direction. This last consideration leads to consider another aspect: the need to isolate the HP accumulator at the exact moment when there is not enough pressure to collect additional fluid, otherwise it would still get a push contrary to the movement of the vehicle.

Superimposing now the three circuits found it get a draft of the complete circuit of figure 53.

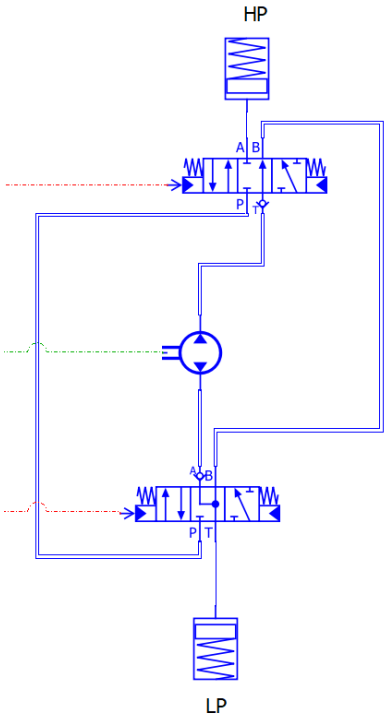

Figure 53: Complete Hydraulic KERS scheme

The proposed scheme considers the adoption of two complex multifunction spool valves, a choice dictated by the need to quickly create a functional model to study its behaviours.

Currently the valves are very articulated and concentrate in two knots several in pressure passages. The first consideration is given by their structure, to contain such a large number of variations leads to mandatory poppet valves, this kind of valves is convenient for the purpose, but they have the defect of having leakages and limited section areas of oil passage with the consequence of generating pressure drops. In the current configuration any method of operation would result in the dissipation of two valves.

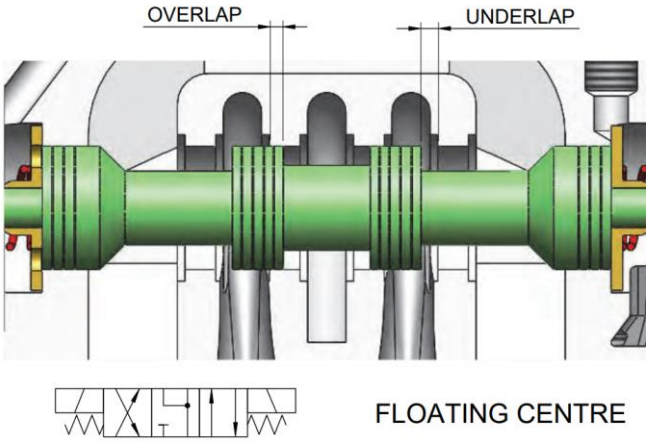

Figure 54: Floating centre spool valve section

In detail, image 55 shows the valve used in the "Top" position, is four-way and three-position, with the non-return valve integrated on the pump line to avoid the spring back effect described above, and the neutral position is in the middle, positions are not progressive and the actuation is piloted.

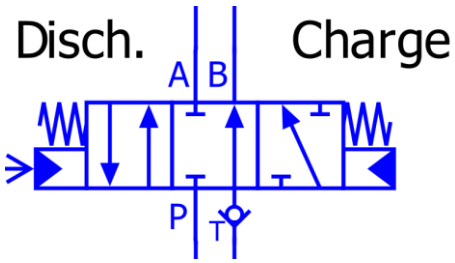

Figure 55: Top position valve

Similarly to the previous one, the valve in the "Bottom" position has the same characteristics of the "Top" valve with the difference of having a "Floating centre" configuration and the non-return valve positioned at the discharge towards the pump, to ensure the presence of fluid on the pump line. The configuration generates the bypass line between A and B in at the neutral position, which is also connected to the LP accumulator to dampening the flow and pressure pulsations.

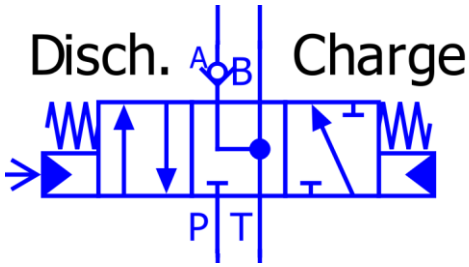

Figure 56: Bottom position valve

The flow section area has been dimensioned with generous dimensions to achieve a lower pressure drop. In the following diagrams in images 57 and 58 it is possible to see the valve opening fractional area.

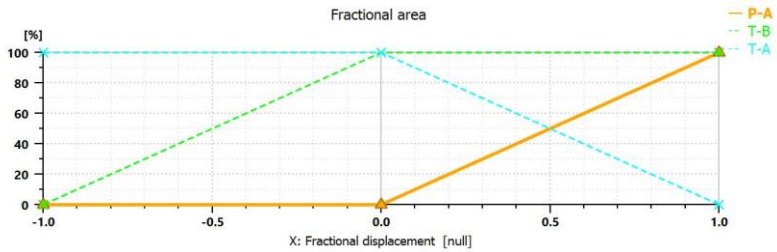

Figure 57: Bottom valve fractional area

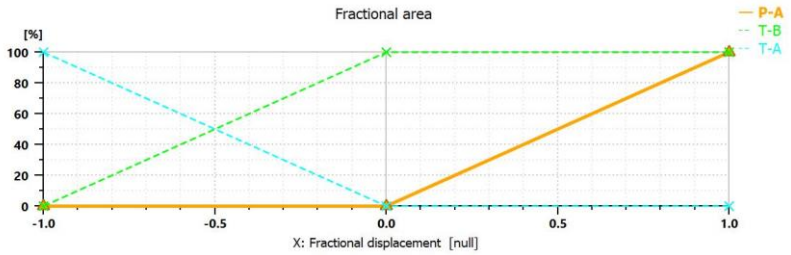

Figure 58: Top valve fractional area

From the simulation whose graph is shown below shows how the results are interesting, they show the desired trend, the system as structured is able to respond correctly to the controls without having abnormal behaviours compared to a traditional bicycle. The only differences are during braking and acceleration with pedal assistance, where there are sharper turns of the curve, which can be resolved with the fine-tuning adjustments of the final product.

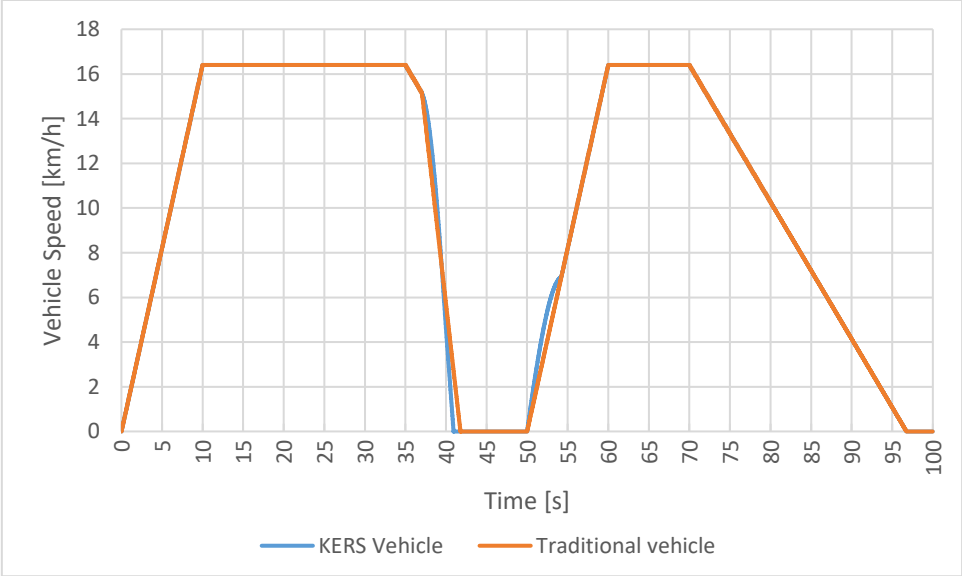

Figure 59: Muscular bike vs KERS bike on standard loop

4.2.3 Simplified model: Circuit with only 2-way valve adoption

Once confirmed that the system was functional, the study phase continued for a more efficient configuration with simpler components. Among the first components to be redesigned are the valves, which was mandatory spool valve until now; this type of valves has the cons of having clearances through which they would be leakages, thus reducing the overall efficiency of the system. The leakages take place in all the overlaps between spool and valve housing for the need to have dimensional tolerances with clearance to facilitate the translation of the spool. So is opted to completely review of the circuit layout in order to adopt only poppet valves, but maintaining the same principles of operation illustrated in the previous paragraph.

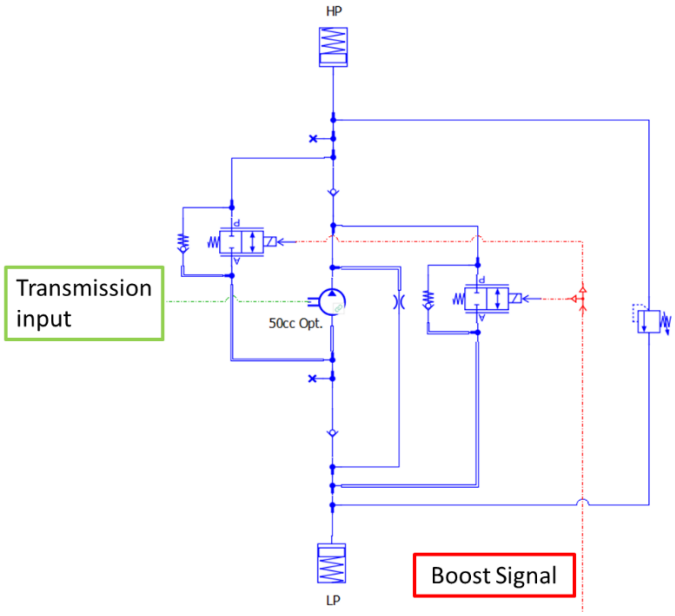

Figure 60: Simplified KERS scheme

The circuit now consists only of non-return valves or driven non-return valves, both are two-way. Which, with a subsequent development phase, could contain the totality of the hydraulic controls under a single valve pack, an example could be for product needs. The octurator of the valve is more effective because the closure is done by use of a conical or spherical body, in the image of example number 61 is coloured with red.

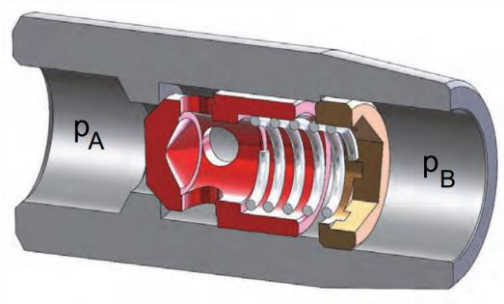

Figure 61: Two-way poppet valve section

Running the simulations again are shows that the overall operation has not changed compared to the previous ones, except for the improvement in terms of dissipated energy through the valves. This valve's structure allows larger passage sections.

Arrived at a level of sufficiently detailed simulation model that, is wanted to calculate the energetic impact of the system on the use of the bicycle. In detail are wanted to compare the energy used in the starting phase from standstill with empty system, or absent, with the same starting conditions but with enough energy stored in the accumulator to restart. To compare in this way the instantaneous power curve in the total time to reaching the same vehicle speed, which means the same amount of kinetic energy. The test cycle includes the phases of empty system acceleration, constant speed rest, short inertial phase, stopping with regeneration and waiting at standstill; then acceleration with energy boost, speed rest again and final inertia stop.

Image 62 shows the speed of the vehicle (in red), the power supplied to the system by the cyclist (in yellow) and the power taken first, and then returned by the hydraulic circuit (in green).

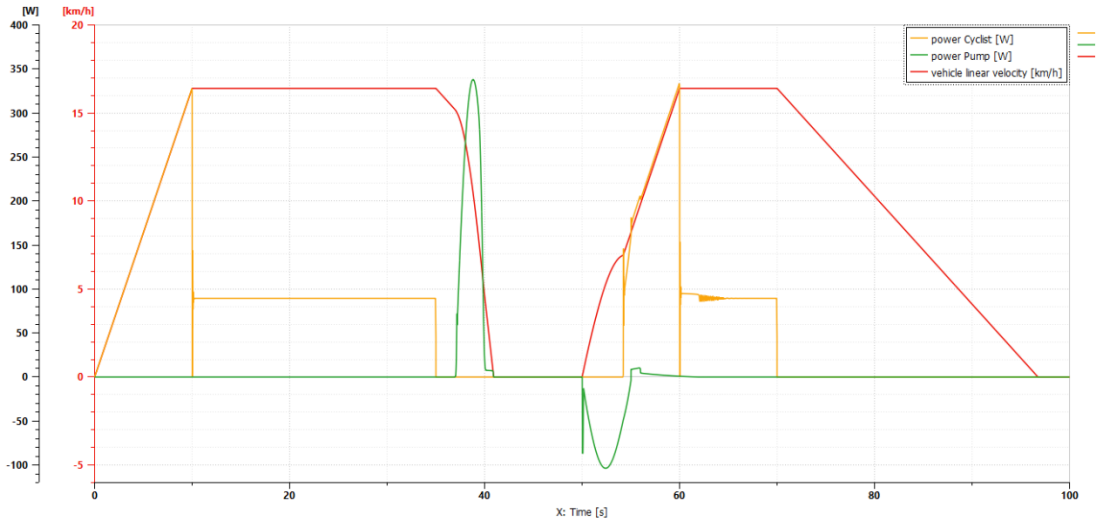

Figure 62: Standard loop test results

The power curve of the two active power phases was extracted: from 0 to 10 seconds and from 50 to 60 seconds. The first has power derived only from the cyclist, the second also records the release by the accumulator until extinction of accumulated energy. With the proposed cycle the energy recovered from braking will be completely exhausted in the next phase of acceleration, allowing the recording of all the accumulated energy. The recorded power is then multiplied by the time interval, the smaller the sampling interval, the more accurate will be the result of the input energy. It is then calculated the difference between energy input during first acceleration and that spent during restart, the calculated energy will be the result of the net kinetic energy given by the efficiency of the accumulation and release, subtracted by the energy dissipated by the vehicle rolling resistance. At the exhaust system, the cyclist had to spend 1644 [J] during the first phase and 1329 [J] during the restart; the difference is quantified in 315 [J], or 19% of the initially energy spent.

The analysis shows that it can save up to 20% of energy for each restart after a braking. Considering that the cyclist will generally use to save energy and to brake as little as possible,

except in conditions that forces the cyclist to an interruption on the route, such as a red light or an obstacle, the percentage of energy saved would be very close to zero, making the system useless, because the active braking phases would be sporadic and minor, while stops for rolling resistance and stop of the vehicle at low power will be very frequent. However, considering the journey time, it is noted that in the case of vehicles with KERS, speeds would tend to increase if used for each stop, encouraging the cyclist to use mainly the braking system with accumulation rather than stop waiting for the extinction of the inertial energy of the bicycle due to the vehicle resistance.

If is imagined a possible market implementation, this system would have to be proposed for all average cyclist and short-term travels. Or for paths with variable and/or constant slope, because the accumulation system with poppet valves would ensure to maintain the pressure even at a distance over time.

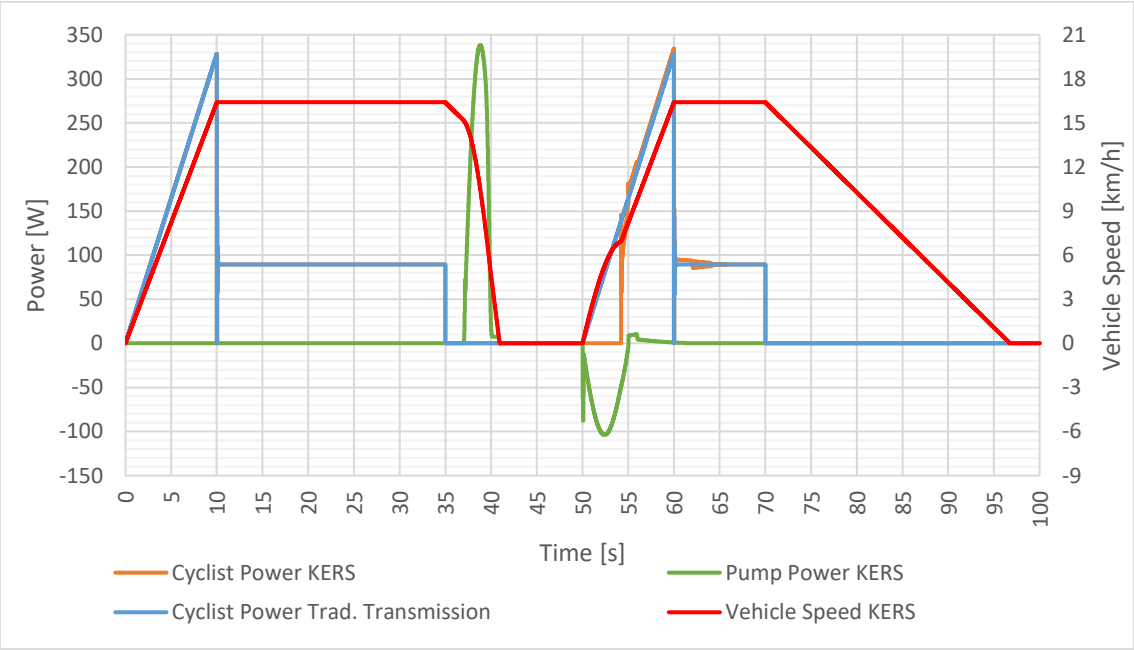

Figure 63: Cyclist power on KERS bike vs Cyclist power on Muscular bike

In addition, it was also verified that the accumulators ware correctly sized for use, of which the graph in figure 64 shows the result. The position of the HP plunger is shown in red, which at the beginning of the regeneration phase is charged without reaching saturation; the charged accumulator is represented by the amount of 0 [mm]. Energy that will be released by the HP accumulator during the restart, returning oil to the LP accumulator, represented in blue; this last one will have the plunger in position 0 [mm] at the beginning of the test and will discharge in braking. Important consideration of sizing is that HP is saturated before emptying LP, to avoid cavitation conditions of the pump during braking.

With the current geometry it is possible to correctly accumulate the energy of the braking and to return it totally to the restart, obviously at net of efficiencies. If the system were to accumulate too much pressure and saturate the HP accumulator, the braking energy would be

completely dissipated, because the pump would generate flow at the pressure of maximum accumulation, dissipating the energy otherwise accumulable.

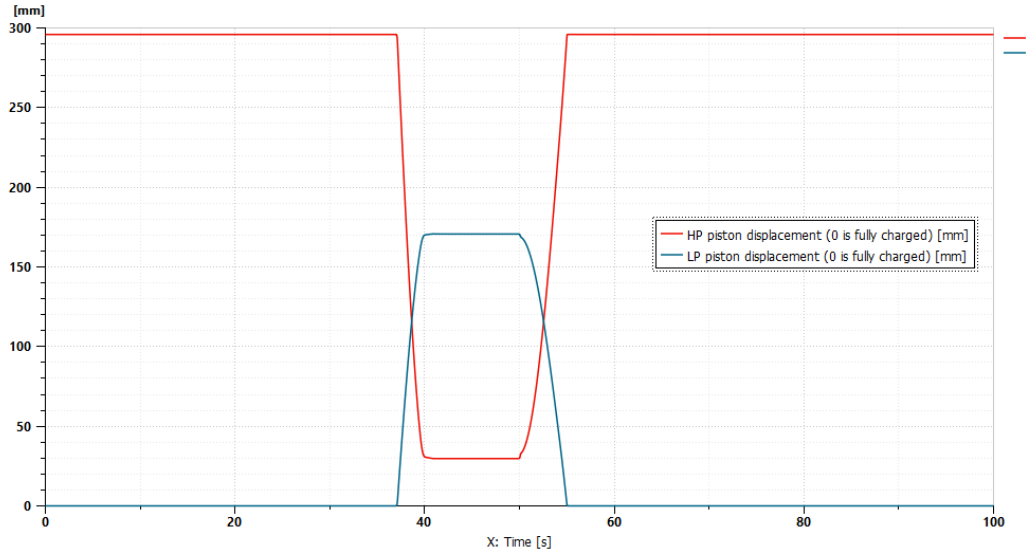

Figure 64: HP and LP accumulator piston position

4.2.4 Considerations

The energy calculation showed that in urban conditions, the accumulation system in braking can give energy saving benefits. Allowing to potentially save of 20% of the energy required at the restart and raise the average vehicle speed, when the braking system would be used more frequently.

Taking a further step in the development it could have to find a solution to implement input commands, the circuit with by-pass could be simpler overall, but with a fixed energy cost. However, it would present a mechanical deactivation of the system when the vehicle is stationary in case of malfunction, with a method of operation similar to the coupling system of a dynamo. Alternatively, the clutch circuit would be mechanically more complex and without energy contraindications, which should include the clutch engagement through the braking control and the possibility of release after the finish of acceleration phase. As a last proposal for future development, the use of a variable displacement hydraulic machine would be evaluated, replacing the current fixed displacement, which would be permanently connected to the transmission replacing the by-pass circuit with the simple zeroing of the displacement and therefore also reducing the dissipated powers. For future investigation the last one proposal would seem to be the most promising.

5. Conclusions

The study has led to a path of analysis that has ranged for numerous versions and alternative interpretations. The original design that had been subjected to the analysis had some shortcomings demonstrating the operativeness, was found a solution with the calculations progression, with a combination of geometric characteristics and structural choose that gave the expected result, making mandatory its modification.

Subsequent at operational demonstration, also subsequent studies of potential alternatives also yielded promising results. The solutions given further deviation from the project presented because it was wanted to show that different interpretations of the same idea would give equally a functional result, which would be competitive for own specific characteristics. As it has been shown that the two-actuator automotive control system has an additional adjustment, which is able to vary the transmission ratio of the bicycle also according to the slope, as well as the speed of travel. In the same way, that the KERS system can lead to energy savings and thus lead to improved comfort while pedaling without having to replace the chain drive.

Bibliography e sitography

1. NERVEGNA N., RUNDO M., Passi nell'Oleodinamica, Epics Edizioni, Collana Politeko, 2020
2. RUNDO M., Automotive Fluid Power Systems, Lecture slides, a.a. 2020-2021
3. GENTA G., Motor Vehicle design, Lecture slides, a.a. 2017-2018
4. RAVELLO V., Electric and Hybrid Propulsion Systems, Lecture slides, a.a. 2020-2021
5. Marinaro G., Xu Z., Chen Z., Li C., Mao Y., Vacca A., The PurdueTracer: An Energy-Efficient Human-Powered Hydraulic Bicycle with Flexible Operation and Software Aids, Pubblicated article January 2018
6. ZEHUS, E-Bike Drivetrain Systems, Commercial Product, Zehus.it - E-Bike
7. B.C. Bike Ltd, OYO chain free bike, Product start up, fundit.co.il - OYO Bike, 2019
8. Van Bon M., Vroemen G., Power Speed Profile: Performance model for road cycling, Pubblicated article, October 2018
9. International Human Powered Vehicle Association, Human Power, Technical journal number 52 Summer 2001
10. Harriger G. A., Hydraulic drive system for bicycles and the like US4546990, United States Patent, October 1985